38. Wen PY, Macdonald DR, Reardon DA, et al. Update response assessment criteria for high-grade gliomas: Response Assessment in Neuro-Oncology Working Group. *J Clin Oncol* 2010;28:1963–72.
39. Vredenburgh JJ, Cloughesy T, Samanto M, et al. Corticosteroid use in patients with glioblastoma at first or second relapse treated with bevacizumab in the BRAIN study. *Oncologist* 2010;15:1329–34.
40. Chamberlain MC, Johnston SK. Salvage therapy with single-agent bevacizumab for recurrent glioblastoma. *J Neurooncol* 2010;96:259–69.
41. *A Study of Avastin (bevacizumab) in Combination with Temozolomide and Radiotherapy in Patients with Newly Diagnosed Glioblastoma [Internet]*. USA: Clinicaltrials.gov, 2009 (cited 4 October 2011). http://clinicaltrials.gov/ct2/show/NCT00943826.
42. *Temozolomide and Radiation Therapy with or Without Bevacizumab in Treating Patients with Newly Diagnosed Glioblastoma [Internet]*. USA: Clinicaltrials.gov, 2009 (cited 4 October 2011). http://clinicaltrials.gov/ct2/show/NCT00884741.
43. Van Meir EG, Hadjipanayis CG, Norden AD, et al. Exciting new advances in neuro-oncology: the avenue to a cure for malignant glioma. *CA Cancer J Clin* 2010;60:166–93.

Cancer Science
The official journal of the Japanese Cancer Association

Importance of direct macrophage - Tumor cell interaction on progression of human glioma

Yoshihiro Komohara,[1,5] Hasita Horlad,[1,5] Koji Ohnishi,[1] Yukio Fujiwara,[1] Bing Bai,[1] Takenobu Nakagawa,[1] Shinya Suzu,[2] Hideo Nakamura,[3] Jun-ichi Kuratsu[3] and Motohiro Takeya[1,4]

[1]Department of Cell Pathology, Graduate School of Medical Sciences, Kumamoto University, Kumamoto; [2]Center for AIDS Research, Kumamoto University, Kumamoto; [3]Department of Neurosurgery, Graduate School of Medical Sciences, Kumamoto University, Kumamoto, Japan

(Received July 10, 2012/Revised August 31, 2012/Accepted September 2, 2012/Accepted manuscript online September 7, 2012/Article first published online October 26, 2012)

We previously showed tumor-associated macrophages/microglia (TAMs) polarized to the M2 phenotype were significantly involved in tumor cell proliferation and poor clinical prognosis in patients with high grade gliomas. However, the detailed molecular mechanisms involved in the interaction between TAMs and tumor cells have been unclear. Current results reveal that, in coculture with human macrophages, BrdU incorporation was significantly elevated in glioma cells, and signal transducer and activator of transcription-3 (Stat3) activation was found in both cell types. Direct mixed coculture led to stronger Stat3 activation in tumor cells than did indirect separate coculture in Transwell chamber dishes. Screening with an array kit for phospho-receptor tyrosine kinases revealed that phosphorylation of macrophage-colony stimulating factor receptor (M-CSFR, CD115, or *c-fms*) is possibly involved in this cell–cell interaction; M-CSFR activation was detected in both cell types. Coculture-induced tumor cell activation was suppressed by siRNA-mediated downregulation of the M-CSFR in macrophages and by an inhibitor of M-CSFR (GW2580). Immunohistochemical analysis of phosphorylated (p) M-CSFR, pStat3, M-CSF, M2 ratio, and MIB-1(%) in high grade gliomas revealed that higher staining of pM-CSFR in tumor cells was significantly associated with higher M-CSF expression and higher MIB-1(%). Higher staining of pStat3 was associated with higher MIB-1(%). High M2 ratios were closely correlated with high MIB-1(%) and poor clinical prognosis. Targeting these molecules or deactivating M2 macrophages might be useful therapeutic strategies for high grade glioma patients. (*Cancer Sci* 2012; 103: 2165–2172)

Macrophages that infiltrate cancer tissues are called tumor-associated macrophages (TAMs) and are closely involved in development of the tumor microenvironment by inducing angiogenesis, immunosuppression, and invasion.[1,2] Tumor-associated macrophages are generally thought to belong to the alternatively activated macrophage population (M2) because of their anti-inflammatory functions.[3] In many kinds of malignant tumors, including melanoma, malignant lymphoma, leiomyosarcoma, pancreatic tumors, intrahepatic cholangiocarcinoma, renal cell carcinoma, and high grade glioma, the presence of M2-polarized TAMs is associated with poor clinical prognosis.[4–11] Although it is well known that many TAMs infiltrate into high grade gliomas and are associated with angiogenesis and immunosuppression,[12–15] results of this study show that M2-polarized TAMs are significantly involved in glioma tumor cell proliferation and are related to poor prognosis of high grade glioma patients.[6]

Signal transducer and activator of transcription-3 (Stat3) affects the tumor microenvironment and tumor development by virtue of its association with immunosuppression, angiogenesis, and cancer cell proliferation.[16,17] In some kinds of malignant tumors, including high grade glioma, patients with high Stat3 activation in tumor cells have significantly worse clinical prognosis.[18] Therefore, Stat3 is thought to be an important target molecule for anticancer therapy, and many researchers have introduced various kinds of Stat3 inhibitors as anticancer drugs.[19] Stat3 signaling in macrophages is known to participate in regulating immune responses. Targeted disruption of Stat3 signaling resulted in activation of antigen-specific T cells, and suppressed tumor development in murine cancer models.[20–22] In patients with glioblastoma, inhibition of Stat3 not only suppressed tumor cell growth but also reversed immune tolerance by impairing the immune-suppressive function of alternatively activated macrophage/microglia.[23]

In this study, M2 macrophages were found to support proliferation of glioma cells through Stat3 activation. Cell–cell interaction during direct contact between tumor cells and macrophages contributes to strong activation of macrophages, which in turn activates tumor cells. *In vitro* results of the use of a receptor-type tyrosine kinase (RTK) array revealed the importance of macrophage-colony stimulating factor receptor (M-CSFR) activation in this cell–cell interaction. The crucial role of macrophage-colony stimulating factor (M-CSF), especially membrane-type M-CSF (mM-CSF), and its binding to M-CSFR during direct cell–cell interactions between tumor cells and macrophages was determined.

Materials and Methods

Macrophage culture. Peripheral blood mononuclear cells were obtained from three healthy volunteer donors and written informed consent for experimental use of the same was supplied by all donors. $CD14^+$ monocytes were isolated using CD14 microbeads (Miltenyi Biotec, Bergisch Gladbach, Germany). Monocytes were plated in 6-well (1×10^5/well) or 12-well (5×10^4/well) plates and cultured with granulocyte M-CSF (2 ng/mL) (Wako, Tokyo, Japan) for 5 days to induce immature macrophages. After PBS washes, cells were stimulated with γ-interferon (1 ng/mL) (PeproTech, Rocky Hill, NJ, USA) to induce M1 macrophages. These cells were stimulated with 50% tumor-cell supernatant (TCS) to induce M2 macrophages, because TCS contains many anti-inflammatory cytokines and pushes macrophage polarization toward the M2 phenotype.[6]

Cell lines. Tumor-cell supernatant was prepared as described previously.[6] The human glioblastoma cell line T98G was purchased from ATCC (Manassas, VA, USA) and was maintained in DMEM supplemented with 10% FBS, 100 U/mL penicillin, 100 μg/mL streptomycin, and 0.1 mg/mL sodium pyruvate. The mycoplasma test was carried out using a PCR detection kit (Takara Bio, Otsu, Japan). Human myeloid leukemia TF-1

[4]To whom correspondence should be addresssed.
E-mail: takeya@kumamoto-u.ac.jp
[5]These authors contributed equally to this work.

doi: 10.1111/cas.12015

cells expressing M-CSFR were cultured in DMEM with 10% FBS and granulocyte M-CSF, as described previously.[24]

Coculture experiment. To investigate the cell cell interaction between tumor cells and macrophages, coculture experiments were carried out as described previously.[25] Briefly, after macrophages were washed in PBS, they were co-incubated with T98G cells for 2 days to evaluate the significance of direct cell cell contact. To examine the influence of indirect cell cell

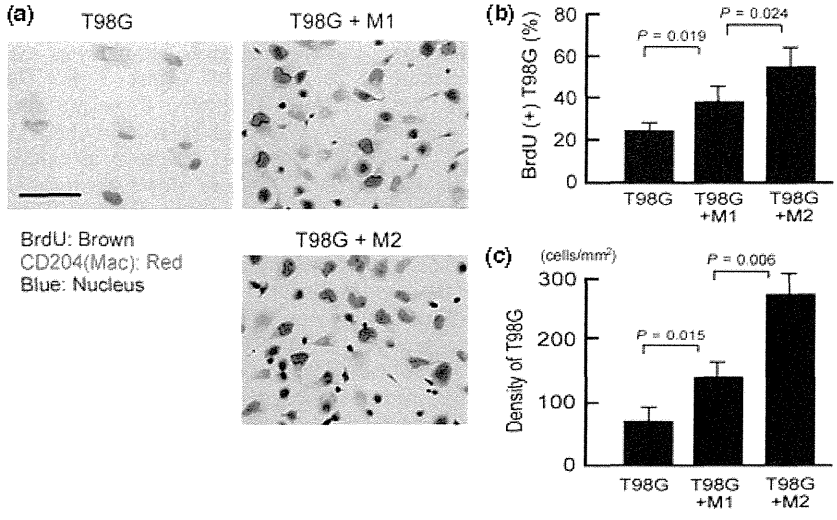

Fig. 1. Tumor cell proliferation by coculture with macrophages. (a) Primary monocyte-derived macrophages were stimulated with γ-interferon (M1) or tumor-cell supernatant (M2), and cocultured with T98G cells for 2 days. Double immunostaining of CD204 and BrdU was carried out to evaluate BrdU incorporation by tumor cells. $CD204^+$ cells (red) indicate macrophages. (b) $BrdU^+$ cells among CD204 tumor cells were counted under a microscope. (c) The number of tumor cells per 1 mm^2 was counted under a microscope.

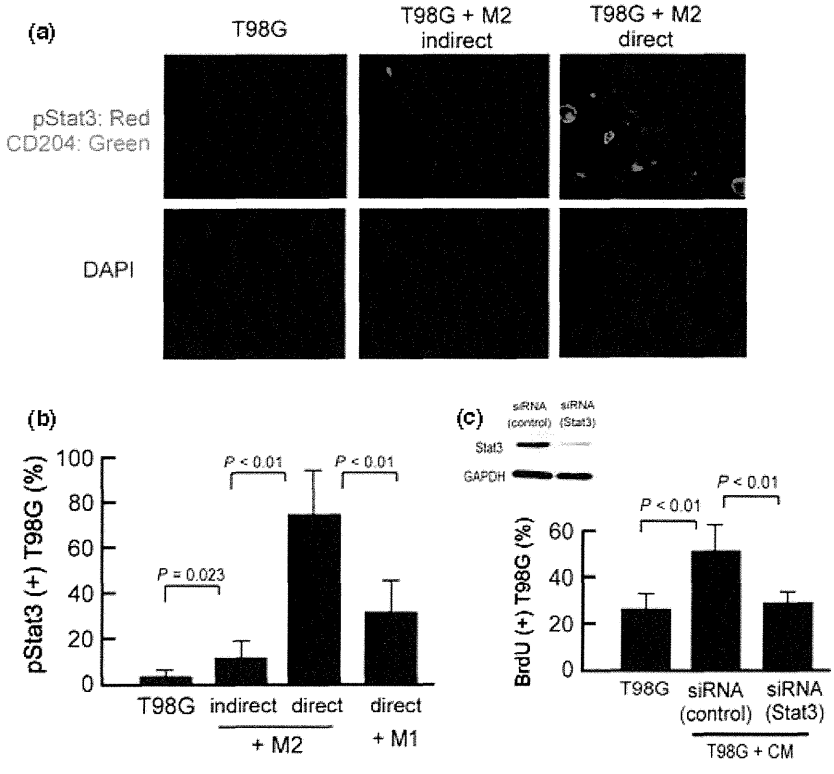

Fig. 2. Signal transducer and activator of transcription-3 (Stat3) activation in cocultured cells. (a) T98G cells were cocultured with tumor-cell supernatant-stimulated M2 macrophages, and Stat3 activation was analyzed by double immunostaining of pStat3 (red) and CD204 (green). Blue indicates nuclear staining. Scale bar = 50 μm. (b) Following double immunostaining, 100 CD204 T98G cells were counted, and the percentage of $pStat3^+$ cells was calculated (n = 3 or 4 for each group). (c) BrdU incorporation in conditional medium-stimulated T98G cells was evaluated with or without Stat3 siRNA. (n = 3 for each group). Downregulation of Stat3 protein in T98G cells was also confirmed by Western blot analysis. (d) Interleukin (IL)-10 production was evaluated as a marker of macrophage activation (n = 4 for each group). (e) Double immunostaining of activated Stat3 (brown) and Iba-1 (marker of macrophages/microglia; blue) was carried out.

doi: 10.1111/cas.12015

interaction, Transwell chamber dishes (Nunc, Rochester, NY, USA) were used.

BrdU incorporation and immunostaining. BrdU incorporation and immunostaining was carried out using the BrdU ELISA kit (Roche, Basel, Switzerland) according to the manufacturer's protocol with minor modifications. Briefly, after culture with BrdU for 90 min, cells were fixed by acetone. CD204 (clone SRA-E5; Transgenic, Kumamoto, Japan) was stained and visualized using the Warp Red chromogen kit (Biocare Medical, Concord, CA, USA). After washes in glycine buffer (pH 2.2), cells were stained with anti-BrdU antibody and visualized using the diaminobenzidine substrate system (Nichirei, Tokyo, Japan).

Immunofluorescence staining of pStat3. Paraffin-embedded cell block specimens were prepared and sectioned as described previously.[25] Mounted sections were deparaffinized in xylene and rehydrated in a graded ethanol series. Following treatment for antigen retrieval, sections were reacted with anti-CD204 antibody (mouse monoclonal, clone SRA-E5) and anti-pStat3 antibody (Tyr705, clone D3A7; Cell Signaling Technology, Denver, MA, USA). Antibodies were diluted with CanGetSignal (Toyobo, Tokyo, Japan). Alexa Fluor 488 goat anti-mouse IgG and Alexa Fluor 546 goat anti-rabbit IgG (Invitrogen, Camarillo, CA, USA) were used as secondary antibodies.

Inhibitor. The M-CSFR inhibitor GW2580 (Calbiochem, Nottingham, UK) was used at either 20 nM or 30 nM concentrations.

Small interfering RNA in human macrophages. Human macrophages were transfected with siRNA against human Stat3 (Santa Cruz Biotechnology, Santa Cruz, CA, USA) or M-CSFR (Santa Cruz Biotechnology) using Lipofectamine RNAi MAX (Invitrogen). Control siRNA (Santa Cruz Biotechnology) was used as a negative control. Downregulation of Stat3 and M-CSFR was evaluated by Western blot and real-time PCR, respectively, as described previously.[9]

Evaluation of cytokine secretion in supernatant. The interleukin (IL)-10 concentration in supernatants was determined using ELISA kits (PeproTech).

Phospho-receptor tyrosine kinase array analysis. The relevant phospho-receptor tyrosine kinase (RTK) array was purchased from R&D Systems (Minneapolis, MN, USA), and used according to the manufacturer's protocol.

Flow cytometry. Cells were detached from wells using enzyme-free Cell Dissociation Buffer (Gibco, Grand Island, NY, USA) and immediately fixed with 4% paraformaldehyde. After incubation with 0.1% saponin, cells were reacted with anti-pM-CSFR antibody and anti-CD68 antibody (mouse monoclonal, clone PM-1K[26]). Then FITC-labeled anti-mouse IgG and phycoerythrin-labeled anti-rabbit IgG were used as secondary antibodies, and cells were analyzed by FACSCalibur.

Human glioblastoma samples. From January 2006 to September 2009, paraffin-embedded tissue samples from 62 patients with high grade gliomas (nine patients with anaplastic astrocytoma and 53 patients with glioblastoma) were prepared for this study. Cases with massive necrosis were not enrolled. Informed written consent was obtained from all patients in accordance with protocols approved by the Kumamoto University Review Board. Tissue samples were fixed in 10% neutral buffered formalin and were embedded in paraffin.[6]

Immunostaining and double immunostaining of surgical specimens. Sections were deparaffinized in xylene and rehydrated in a graded ethanol series. Anti-pStat3 antibody (clone D3A7; Cell Signaling Technology), anti-pM-CSFR antibody (Tyr 723, clone 49C10; Cell Signaling Technology), anti-M-CSF antibody (clone EP1179Y; Novus Biologicals, Littleton, CO, USA), anti-CD163 antibody (clone 10D6; Novocastra, Newcastle, UK), anti-Iba-1 (polyclonal; Wako), and anti-Ki-67 (clone MIB-1; Dako, Glostrup, Denmark) were used as primary antibodies. Horseradish peroxidase-labeled or alkaline phosphatase-labeled antibodies (Nichirei) were used as secondary antibodies. Reactions were visualized by the diaminobenzidine system (Nichirei), Fast Blue solution (Sigma, St. Louis, MO, USA), or HistoGreen (Linaris Biologische, Wertheim-Bettingen, Germany). Macrophage-colony stimulating factor receptor activation and M-CSF expression was scored as 0 (negative), 1 (weak), or 2 (strong) by two pathologists (Y.K. and H.H.) who were blind to the sample data, then the sum of scores for each sample was categorized as "low" (score 0 2) or "high" (score 3 4). The MIB-1 index and M2 ratio ($CD163^+$ cells/$Iba\text{-}1^+$ cells) were determined by two pathologists (Y.K. and H.H.) and the values obtained were averaged. Because a previous study showed that the ratio of $CD163^+$ TAMs is closely correlated with tumor cell proliferation and clinical prognosis,[6] patients were divided into two M2 ratio groups, low (<30%) and high (> 30%). Stat3 activation was scored as 0 to 8 as described previously,[27] then the sum of scores for each sample was categorized as "low" (score 0 4) or "high" (score 5 8).

Statistics. Statistical analysis of *in vitro* and *in vivo* data was carried out using JMP10 (SAS Institute, Chicago, IL, USA). All data from *in vitro* studies represent results of two or three independent experiments. Data are expressed as the mean ± SD. The Mann Whitney *U*-test was used for two-group comparisons. A value of $P < 0.05$ was considered statistically significant.

Results

Glioblastoma cells were activated by coculture with M2 macrophages. In the first experiments, the effects of cell cell interaction between macrophages and T98G cells were investigated by means of the coculture system. BrdU incorporation into T98G cells was evaluated by double immunostaining, and was found to be significantly upregulated by coculture with macrophages; M2, rather than M1, cells caused a notable increase of BrdU incorporation by T98G cells (Fig. 1a,b).

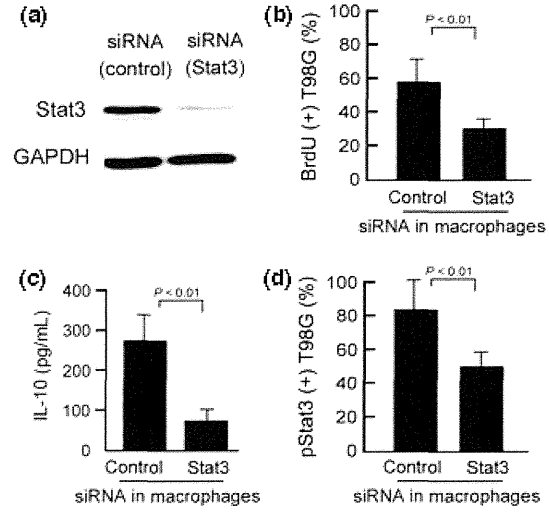

Fig. 3. Effect of selective signal transducer and activator of transcription-3 (Stat3) silencing in macrophages on Stat3 activation in glioma cells. (a) Western blot analysis confirmed suppression of Stat3 in macrophages. (b) Two days after suppression of Stat3 in macrophages, T98G cells were added to the culture. After coculture for 2 days, double immunostaining of CD204 and BrdU was carried out. Percentages of $BrdU^+$ cells among CD204 tumor cells were calculated. (c) In the same conditions, interleukin (IL)-10 concentration in supernatants was determined. (d) After the same treatment, cells were prepared as cell block specimens and double immunostaining of CD204 and pStat3 was done. Percentages of $pStat3^+$ cells among the CD204 tumor cells were calculated.

The proliferation of T98G cells was increased by coculture with M1 and M2, but notably higher proliferation was induced by M2 (Fig. 1c).

As Stat3 is one of the signaling molecules related to cell proliferation and survival, Stat3 activation was evaluated in the coculture system. When M2 cells and T98G cells were cocultured, both cell types showed strong nuclear staining of pStat3 (Fig. 2a,b). In contrast to indirect coculture conditions, direct cell cell interaction caused significantly stronger Stat3 activation in cancer cells (Fig. 2b). Stat3 activation in T98G cells was more strongly induced by coculture with M2 cells compared with M1 cells (Fig. 2b). The proliferation of T98G cells was induced by stimulation with conditional medium of cocultured M2 cells and T98G cells, and this effect was significantly suppressed by blocking Stat3 in T98G cells (Fig. 2c).

To evaluate macrophage activation in the coculture system, IL-10 concentrations in supernatants were determined, because no IL-10 secretion was detected in supernatants of T98G cell monocultures. As shown in Figure 2(d), IL-10 secretion was induced by coculture and, notably, direct coculture induced significantly increased IL-10 secretion. We next evaluated Stat3 activation in human glioma tissues. Among 12 high grade glioma samples analyzed, 10 showed distinct infiltration of $pStat3^+$ TAMs (Fig. 2e). These observations indicate a critical role for Stat3 in cell cell interaction between tumor cells and macrophages.

Activation of Stat3 involved in cell cell interaction between glioma cells and macrophages. We next suppressed Stat3 in M2 macrophages using siRNA before coculture with T98G cells to ascertain whether Stat3 activation in macrophages contributes

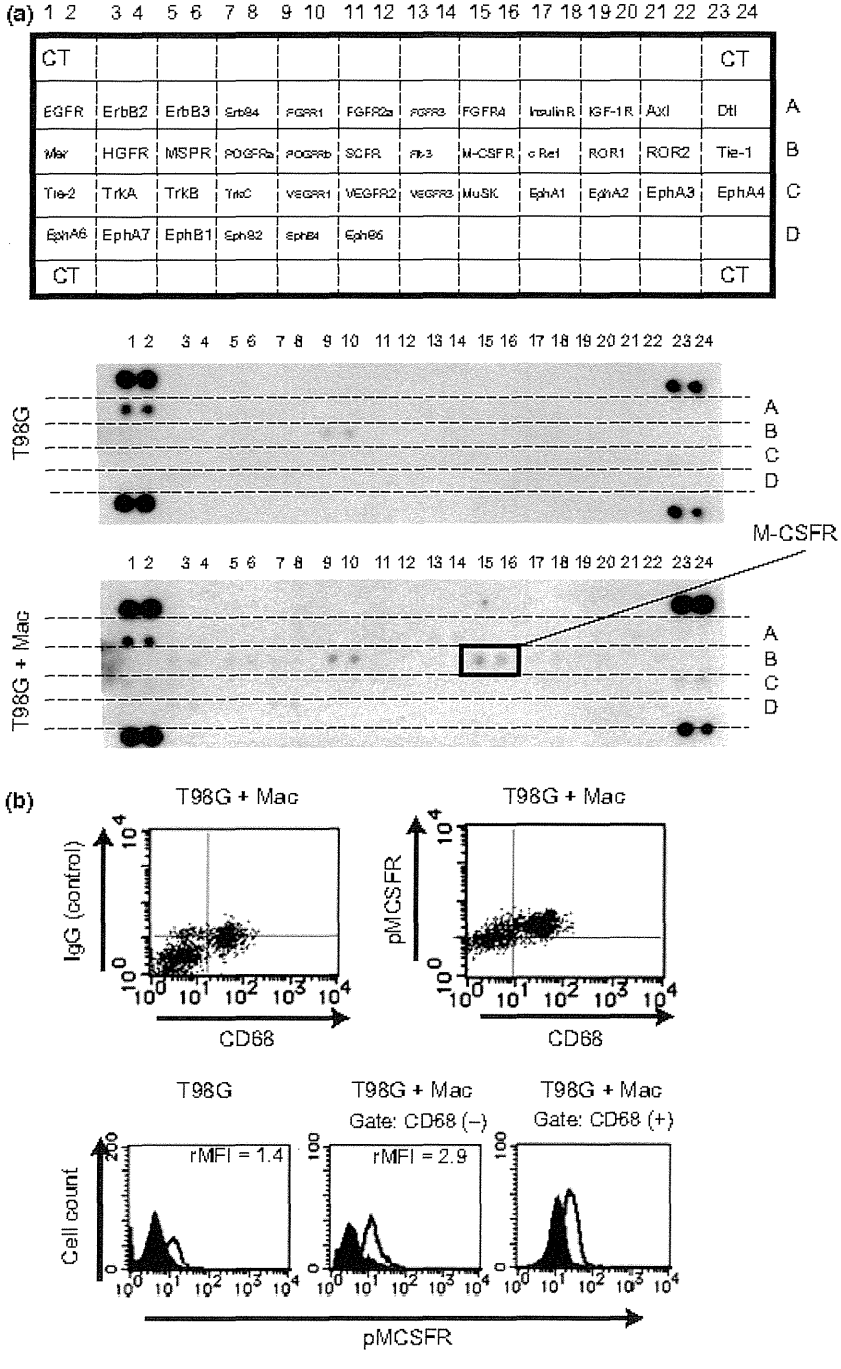

Fig. 4. Receptor-type tyrosine kinase array and flow cytometry. (a) Receptor-type tyrosine kinase array analyses were carried out and results for cocultured cells (T98G + Mac) and T98G cells in monoculture (T98G) were compared. CT, positive control. (b) Phosphorylation of macrophage colony-stimulating factor receptor (M-CSFR) was evaluated by flow cytometry. Representative data from one of two experiments.

doi: 10.1111/cas.12015

to the cell cell interaction (Fig. 3a,b). Incorporation of BrdU into T98G cells was significantly inhibited by Stat3 suppression in macrophages (Fig. 3b). Secretion of IL-10 from macrophages was also inhibited by Stat3 suppression (Fig. 3c). As Figure 3(d) shows, Stat3 activation in T98G cells was decreased by blocking Stat3 in macrophages. These data indicate that macrophage activation through Stat3 signaling is important for tumor cell activation in coculture.

Activation of M-CSFR involved in cell cell interaction. Direct contact with tumor cells significantly induced macrophage activation. Therefore, we hypothesized that RTK mediates this effect, and RTK array analysis was carried out. Activation of RTK in cocultured cells was compared with that of macrophages and T98G cells cultured separately, and significant activation of M-CSFR was found in cocultured macrophages (Fig. 4a), as well as, interestingly, in the cocultured T98G cells (Fig. 4b).

Activation of M-CSFR involved in macrophage activation by direct cell cell interaction, and induced Stat3 activation in tumor cells. Next, we investigated whether M-CSFR is involved in

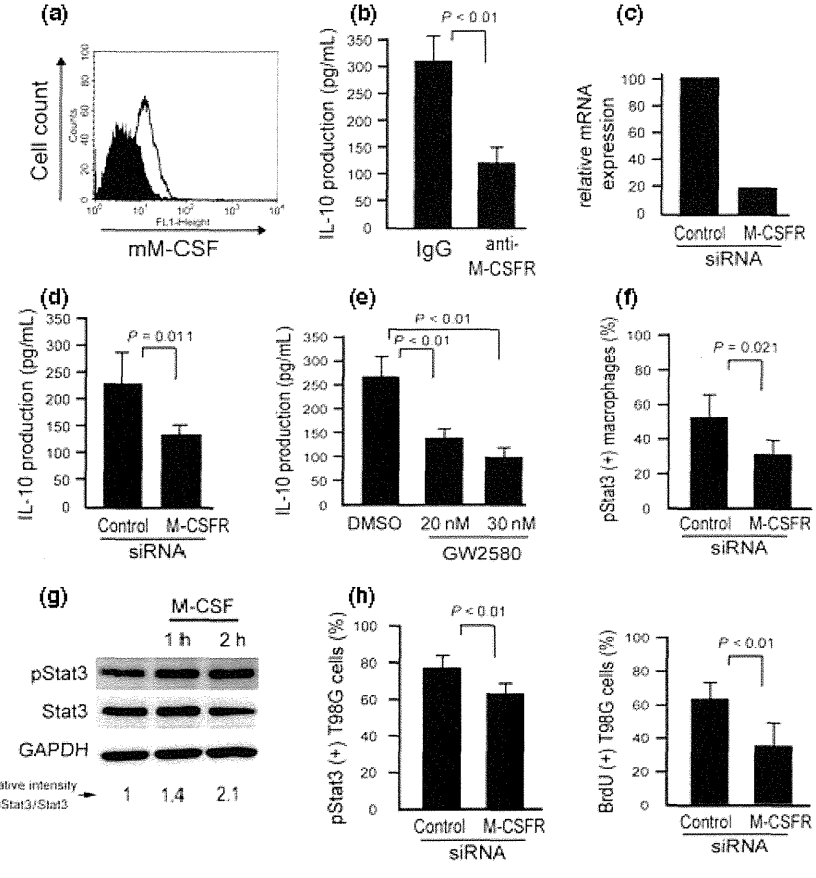

Fig. 5. Involvement of macrophage colony-stimulating factor receptor (M-CSFR) in direct cell–cell interaction. (a) Membrane-type M-CSF (mM-CSF) was expressed on the surface membranes of T98G cells. (b) T98G cells were cocultured with macrophages in the presence of anti-M-CSF antibody for 2 days, and interleukin (IL)-10 in the supernatant was measured by ELISA. Non-immunized rabbit IgG was used as the control. (c) Downregulation of M-CSFR by siRNA was confirmed by real-time PCR. (d) T98G cells were cocultured with macrophages having silenced M-CSFR for 2 days, and IL-10 in the supernatant was measured. (e) Macrophages and T98G cells were mixed and cultured with the M-CSFR inhibitor GW2580 for 2 days, and IL-10 in the supernatant was measured. (f) M-CSFR of macrophages was silenced by siRNA, and coculture proceeded for 2 days. Signal transducer and activator of transcription-3 (Stat3) activation in macrophages was evaluated by double immunostaining. (g) Macrophages were stimulated with M-CSF (100 ng/mL) for 1 or 2 h, and Stat3 activation was evaluated. (h) M-CSFR of macrophages was silenced by siRNA, and coculture proceeded. BrdU incorporation and Stat3 activation in T98G cells was examined by double immunostaining (n = 3 or 4 for each group).

Table 1. Clinicopathologic factors, macrophage-colony stimulating factor receptor (M-CSFR) activation, macrophage-colony stimulating factor (M-CSF) expression, and signal transducer and activator of transcription-3 (Stat3) activation in high grade glioma

Variable	n	M-CSFR activation		P-value	M-CSF expression		P-value	Stat3 activation		P-value
		Low	High		Low	High		Low	High	
Age, years										
<60	26	15	11	P = 0.700	12	14	P = 0.760	11	15	**P = 0.025**
≥60	36	19	17		18	18		6	30	
Gender										
Male	40	18	22	**P = 0.036**	18	22	P = 0.470	8	32	P = 0.077
Female	22	16	6		12	10		9	13	
M-CSFR activation										
Low	33	–	–	–	25	8	**P < 0.001**	11	22	P = 0.270
High	29	–	–		3	26		6	23	
M-CSF expression										
Low	30	–	–	–	–	–	–	10	20	P = 0.310
High	32	–	–		–	–		7	25	
M2 macrophages										
Low	25	15	10	P = 0.27	17	8	**P = 0.011**	9	16	P = 0.210
High	37	17	20		13	24		8	29	

Bold text indicates statistically significant results, calculated using the chi-squared test.

Table 2. Univariate Cox regression analysis of potential prognostic factors

		Univariate analysis		
	n	Mean survial (weeks)	*P*-value Log–rank	*P*-value Wilcoxon
Age, years				
<60	26	88	**0.034**	**0.006**
≥60	36	57		
Gender				
Male	40	72	0.42	0.91
Female	22	65		
pM-CSFR				
Low	34	78	0.054	0.089
High	28	64		
M-CSF				
Low	33	72	0.49	0.57
High	29	65		
Stat3 activation				
Low	17	124	0.058	0.22
High	45	85		
M2 ratio				
Low	25	98	0.003	0.004
High	37	62		
MIB-1 (%)				
<30	26	113	0.0005	0.0007
≥30	36	56		

Bold text indicates statistically significant results. M-CSF, macrophage-colony stimulating factor; pM-CSFR, phosphorylated M-CSF receptor; MIB-1, anti-Ki-67; Stat3, transducer and activator of transcription-3.

macrophage activation by coculture with T98G cells. The T98G cells expressed mM-CSF on their cell surface membranes (Fig. 5a). Neutralizing antibody for mM-CSF and silencing of M-CSFR significantly inhibited IL-10 secretion in direct coculture (Fig. 5b d). An inhibitor of M-CSFR (GW2580) also suppressed IL-10 secretion (Fig. 5e). Activation of Stat3 was inhibited by silencing M-CSFR in macrophages (Fig. 5f) and was significantly induced by M-CSF stimulation in macrophages (Fig. 5g). These data indicate that M-CSFR signaling contributes to Stat3 activation in cocultured macrophages.

We then tested if M-CSFR signaling in macrophages influences tumor cell activation. Both BrdU incorporation and Stat3 activation in cocultured tumor cells were decreased by silencing M-CSFR in macrophages (Fig. 5h).

M2 ratio and M-CSFR activation associated with MIB-1 index in high grade glioma. Immunostaining for pM-CSFR, M-CSF, CD163, Iba-1, and MIB-1 was carried out in 62 cases of high grade glioma. Mutual correlations of their expression and the association with clinical prognosis were statistically evaluated (Tables 1,2). The specificity of anti-pM-CSFR antibody was confirmed using M-CSFR-expressing TF-1 histiocytic cells (Fig. 6a). Both M-CSF expression and M-CSFR activation, as well as M2 phenotype, were classified into two groups, high and low, as described above (Fig. 6b). A positive pM-CSFR signal was seen in both tumor cells and macrophages (Fig. 6c). Activation of Stat3 was also classified into two groups (Fig. 6d). Higher activation of M-CSFR in tumor cells was closely associated with higher M-CSF expression and a higher MIB-1 (%) (Table 1, Fig. 6d). A higher M2 ratio ($CD163^+$ cells/$Iba\text{-}1^+$ cells), higher M-CSF expression, and higher Stat3 activation was also correlated with a higher MIB-1(%) (Fig. 6e). In addition, the patients with higher ages, M2 ratios, or MIB-1(%) had statistically significant shorter survival

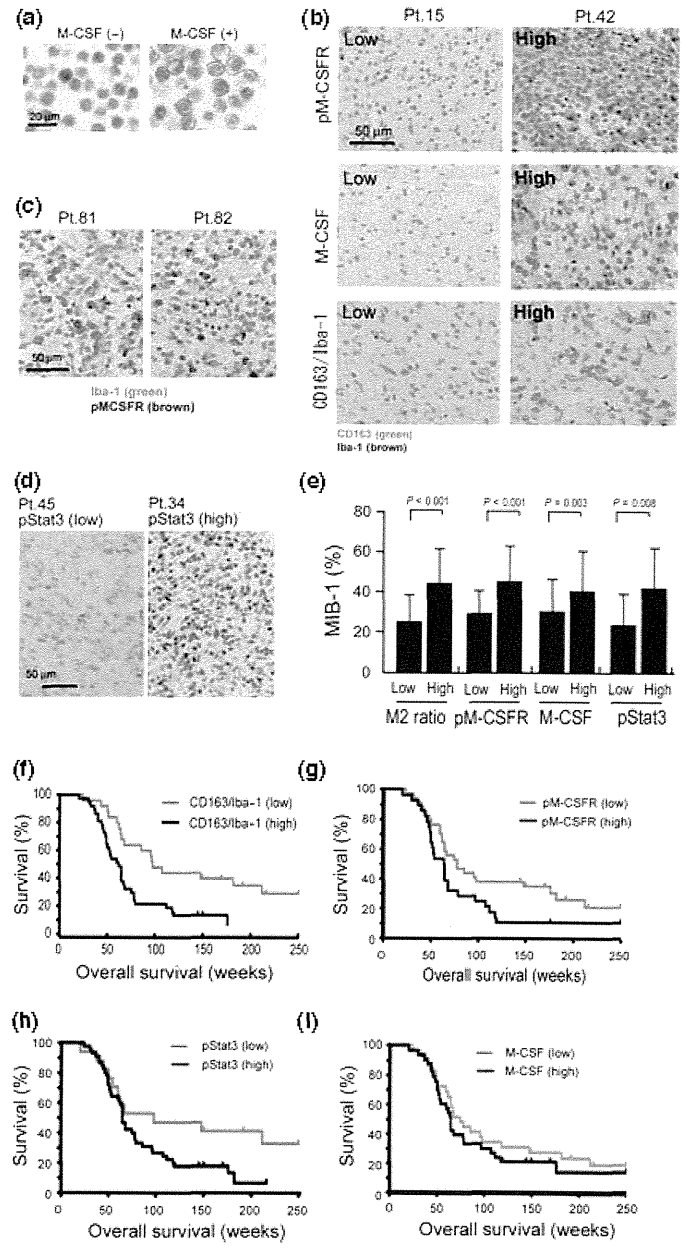

Fig. 6. Immunohistochemical determination of phosphorylated macrophage-colony stimulating factor receptor (pM-CSFR), macrophage-colony stimulating factor (M-CSF), phosphorylated signal transducer and activator of transcription-3 (pStat3), anti-Ki-67 (clone MIB-1), and M2 ratios in human high grade gliomas. (a) TF-1 culture cells were stimulated by M-CSF for 5 min and activation of M-CSFR was evaluated by immunostaining with anti-pM-CSFR. Strong activation of pM-CSFR was detected on cell surfaces of M-CSF-stimulated TF-1 cells. (b) Immunostaining of pM-CSFR, M-CSF, and double immunostaining of CD163 (green) and Iba-1 (brown) were carried out. Results for patient (Pt.) no. 15 and no. 42 are shown. (c) By double immunostaining ofIba-1 (green) and pM-CSFR (brown), pM-CSFR was detected in both tumor cells and macrophages. (d) Immunostaining of pStat3 was also carried out to evaluate the Stat3 activation in tumor cells. (e) M2 ratio, M-CSFR activation, Stat3 activation, and M-CSF expression were correlated with the MIB-1 index. The Kaplan–Meier method was used to determine (f) M2 ratio, (g) M-CSFR activation, (h) Stat3 activation and (i) M-CSF expression.

periods (Fig. 6f, Table 2). The patients with higher M-CSFR and Stat3 activation had shorter survival periods, but this result was not statistically significant (Fig. 6g,h). In

doi: 10.1111/cas.12015

addition, M-CSF expression was not significantly associated to clinical prognosis (Fig. 6i).

Discussion

The importance of TAMs in tumor growth has been well documented, and TAMs are thought to contribute to tumor progression and invasion.[28,29] In this study, we showed that direct contact with glioma cells induces macrophage activation, which in turn activates tumor cells. Macrophage activation through M-CSFR/Stat3 signaling was shown to play an important role in cell–cell interaction. Analysis of human glioma samples indicated that M-CSFR activation and M2 ratios are associated with tumor cell proliferation.

The importance of direct cell–cell contact in cell–cell interaction has been a focus for several researchers. Direct cell–cell contact between macrophages and tumor cells protected tumor cells from chemotherapy drug-induced apoptosis, whereas cell–cell interaction without direct contact did not.[30] A previous study showed that Stat3 activation in ovarian and kidney cancer cells was significantly induced by direct coculture with macrophages.[9,25] As Stat3 is associated with cancer cell proliferation and survival,[16,17] macrophages are thought to support cancer cell proliferation and survival in patients with malignant tumors. A selective Stat3 inhibitor and Stat3 siRNA reversed cytokine expression levels and suppressed tumor growth *in vivo*, and this indicated a major contribution of Stat3 signaling in the immunosuppression by glioma-derived factors.[31,32]

It is well known that mM-CSF induces stronger activation of M-CSFR than soluble M-CSF, although details of the mechanisms involved have been unclear.[33,34] In this study, the possible involvement of mM-CSF–M-CSFR binding on strong Stat3 activation in tumor microenvironment was shown. It is well known that M-CSFR signaling activates some signal molecules including Stat3 activation,[35] and the results shown in Figure 5 indicate that M-CSFR signaling was significantly related to Stat3 activation in this coculture system. Stat3 activation plays an important role in maintenance of glioma stem cells (GSCs),[36] and unknown Stat3-related cytokines derived from GSCs induce macrophage polarization into the M2 phenotype.[37] Although M-CSF expression in GSCs has, to the best of our knowledge, never been reported, the current results suggest that cell–cell interaction between macrophages and GSCs is involved in creating the stem-cell niche of high grade gliomas.

Some studies have shown the efficacy of M-CSFR inhibitors in murine cancer models. Recently, the M-CSFR inhibitor Ki20227 was shown to suppress tumor angiogenesis, lymphangiogenesis, and metastasis, and these effects were suggested to be caused by macrophage dysfunction.[38] GW2580 inhibited the recruitment of myeloid cells into tumor tissues and combination therapy with an anti-angiogenic agent significantly suppressed tumor growth.[39,40] These data indicate that blocking of M-CSFR is effective as an anticancer therapy through abrogating the functions of myeloid cells.

In a previous study, we showed that the M2 ratio of TAMs is significantly associated with high tumor cell proliferation and poor clinical prognosis in patients with high grade glioma.[6] As shown in Figure 6, the current study indicated that poor clinical prognosis was statistically significantly associated with higher M2 ratio, higher age, and higher MIB-1(%), confirming observations consistent with the previous study. In addition, M-CSFR activation in tumor cells was correlated with M-CSF expression and MIB-1(%) but not macrophage phenotype. These findings indicate that further studies are necessary to elucidate detailed mechanisms underlying the effects of cell–cell interaction in the glioma microenvironment.

Results showing that blocking M-CSFR and Stat3 in macrophages suppressed tumor cell activation indicate that some soluble factors derived from activated macrophages contribute to tumor cell activation in coculture experiments. Although we were not able to identify macrophage-derived soluble factors, it was previously reported that glioma-derived factors enhanced Stat3 activity in microglia, and induced increased production of transforming growth factor-β, IL-6, and IL10 in a murine model.[31] A selective Stat3 inhibitor and Stat3 siRNA reversed cytokine expression levels and suppressed tumor growth *in vivo*, indicating a major contribution of Stat3 signaling to immunosuppression by glioma-derived factors.[31,32]

In summary, results of the present study indicate that macrophage activation through M-CSFR/Stat3 signals plays an important role in cell–cell interaction between macrophages and tumor cells. The M-CSFR/Stat3 signals might be potential targets for therapeutic inhibition of macrophage-related cell–cell interaction, an approach that may well prove promising for patients with high grade glioma.

Acknowledgments

We thank Ms Emi Kiyota, Mr Osamu Nakamura, and Ms Yui Hayashida (Department of Cell Pathology, Kumamoto University) for their technical assistance. This study was supported in part by Grants-in-Aid for Scientific Research (B20390113, 21790388) from the Ministry of Education, Culture, Sports, Science, and Technology of Japan.

Disclosure Statement

The authors have no conflict of interest.

References

1 Pollard JW. Tumour-educated macrophages promote tumour progression and metastasis. *Nat Rev Cancer* 2004; **4**: 71 8.
2 Sica A, Schioppa T, Mantovani A, Allavena P. Tumour-associated macrophages are a distinct M2 polarised population promoting tumour progression: potential targets of anti-cancer therapy. *Eur J Cancer* 2006; **42**: 717 27.
3 Gordon S. Alternative activation of macrophages. *Nat Rev Immunol* 2003; **3**: 23 35.
4 Jensen TO, Schmidt H, Moller HJ *et al.* Macrophage markers in serum and tumor have prognostic impact in American Joint Committee on Cancer stage I/II melanoma. *J Clin Oncol* 2009; **27**: 3330 7.
5 Espinosa I, Beck AH, Lee CH *et al.* Coordinate expression of colony-stimulating factor-1 and colony-stimulating factor-1-related proteins is associated with poor prognosis in gynecological and nongynecological leiomyosarcoma. *Am J Pathol* 2009; **174**: 2347 56.
6 Komohara Y, Ohnishi K, Kuratsu J, Takeya M. Possible involvement of the M2 anti-inflammatory macrophage phenotype in growth of human gliomas. *J Pathol* 2008; **216**: 15 24.
7 Kurahara H, Shinchi H, Mataki Y *et al.* Significance of M2-polarized tumor-associated macrophage in pancreatic cancer. *J Surg Res* 2009; **167**: e211 9.
8 Hasita H, Komohara Y, Okabe H *et al.* Significance of alternatively activated macrophages in patients with intrahepatic cholangiocarcinoma. *Cancer Sci* 2010; **101**: 1913 9.
9 Komohara Y, Hasita H, Ohnishi K *et al.* Macrophage infiltration and its prognostic relevance in clear cell renal cell carcinoma. *Cancer Sci* 2011; **102**: 1424 31.
10 Niino D, Komohara Y, Murayama T *et al.* Ratio of M2 macrophage expression is closely associated with poor prognosis for Angioimmunoblastic T-cell lymphoma (AITL). *Pathol Int* 2010; **60**: 278 83.
11 Steidl C, Lee T, Shah SP *et al.* Tumor-associated macrophages and survival in classic Hodgkin's lymphoma. *N Engl J Med* 2010; **362**: 875 85.

12 Nishie A, Ono M, Shono T *et al.* Macrophage infiltration and heme oxygenase-1 expression correlate with angiogenesis in human gliomas. *Clin Cancer Res* 1999; **5**: 1107 13.
13 Hirano H, Tanioka K, Yokoyama S, Akiyama S, Kuratsu J. Angiogenic effect of thymidine phosphorylase on macrophages in glioblastoma multiforme. *J Neurosurg* 2001; **95**: 89 95.
14 Hussain SF, Yang D, Suki D, Aldape K, Grimm E, Heimberger AB. The role of human glioma-infiltrating microglia/macrophages in mediating antitumor immune responses. *Neuro Oncol* 2006; **8**: 261 79.
15 Zhai H, Heppner FL, Tsirka SE. Microglia/macrophages promote glioma progression. *Glia* 2011; **59**: 472 85.
16 Yu H, Kortylewski M, Pardoll D. Crosstalk between cancer and immune cells: role of STAT3 in the tumour microenvironment. *Nat Rev Immunol* 2007; **7**: 41 51.
17 Yoshimura A. Signal transduction of inflammatory cytokines and tumor development. *Cancer Sci* 2006; **97**: 439 47.
18 Abou-Ghazal M, Yang DS, Qiao W *et al.* The incidence, correlation with tumor-infiltrating inflammation, and prognosis of phosphorylated STAT3 expression in human gliomas. *Clin Cancer Res* 2008; **14**: 8228 35.
19 Page BD, Ball DP, Gunning PT. Signal transducer and activator of transcription 3 inhibitors: a patent review. *Expert Opin Ther Pat* 2011; **21**: 65 83.
20 Cheng F, Wang HW, Cuenca A *et al.* A critical role for Stat3 signaling in immune tolerance. *Immunity* 2003; **19**: 425 36.
21 Wu L, Du H, Li Y, Qu P, Yan C. Signal transducer and activator of transcription 3 (Stat3C) promotes myeloid-derived suppressor cell expansion and immune suppression during lung tumorigenesis. *Am J Pathol* 2011; **179**: 2131 41.
22 Fujita M, Kohanbash G, Fellows-Mayle W *et al.* COX-2 blockade suppresses gliomagenesis by inhibiting myeloid-derived suppressor cells. *Cancer Res* 2011; **71**: 2664 74.
23 Hussain SF, Kong LY, Jordan J *et al.* A novel small molecule inhibitor of signal transducers and activators of transcription 3 reverses immune tolerance in malignant glioma patients. *Cancer Res* 2007; **67**: 9630 6.
24 Chihara T, Suzu S, Hassan R *et al.* IL-34 and M-CSF share the receptor Fms but are not identical in biological activity and signal activation. *Cell Death Differ* 2010; **17**: 1917 27.
25 Takaishi K, Komohara Y, Tashiro H *et al.* Involvement of M2-polarized macrophages in the ascites from advanced epithelial ovarian carcinoma in tumor progression via Stat3 activation. *Cancer Sci* 2010; **101**: 2128 36.
26 Horikawa T, Komohara Y, Kiyota E, Terasaki Y, Takagi K, Takeya M. Detection of guinea pig macrophages by a new CD68 monoclonal antibody, PM-1K. *J Mol Histol* 2006; **37**: 15 25.
27 Komohara Y, Horlad H, Ohnishi K *et al.* M2 macrophage/microglial cells induce activation of Stat3 in primary central nervous system lymphoma. *J Clin Exp Hematop* 2011; **51**: 93 9.
28 Sica A, Mantovani A. Macrophage plasticity and polarization: in vivo veritas. *J Clin Invest* 2012; **122**: 787 95.
29 Baay M, Brouwer A, Pauwels P, Peeters M, Lardon F. Tumor cells and tumor-associated macrophages: secreted proteins as potential targets for therapy. *Clin Dev Immunol* 2011; **2011**: 565187.
30 Zheng Y, Cai Z, Wang S *et al.* Macrophages are an abundant component of myeloma microenvironment and protect myeloma cells from chemotherapy drug-induced apoptosis. *Blood* 2009; **114**: 3625 8.
31 Zhang L, Alizadeh D, Van Handel M, Kortylewski M, Yu H, Badie B. Stat3 inhibition activates tumor macrophages and abrogates glioma growth in mice. *Glia* 2009; **57**: 1458 67.
32 Fujita M, Zhu X, Sasaki K *et al.* Inhibition of STAT3 promotes the efficacy of adoptive transfer therapy using type-1 CTLs by modulation of the immunological microenvironment in a murine intracranial glioma. *J Immunol* 2008; **180**: 2089 98.
33 Douglass TG, Driggers L, Zhang JG *et al.* Macrophage colony stimulating factor: not just for macrophages anymore! A gateway into complex biologies. *Int Immunopharmacol* 2008; **8**: 1354 76.
34 Stein J, Borzillo GV, Rettenmier CW. Direct stimulation of cells expressing receptors for macrophage colony-stimulating factor (CSF-1) by a plasma membrane-bound precursor of human CSF-1. *Blood* 1990; **76**: 1308 14.
35 Novak U, Harpur AG, Paradiso L *et al.* Colony-stimulating factor 1-induced STAT1 and STAT3 activation is accompanied by phosphorylation of Tyk2 in macrophages and Tyk2 and JAK1 in fibroblasts. *Blood* 1995; **86**: 2948 56.
36 Sherry MM, Reeves A, Wu JK, Cochran BH. STAT3 is required for proliferation and maintenance of multipotency in glioblastoma stem cells. *Stem Cells* 2009; **27**: 2383 92.
37 Wu A, Wei J, Kong LY *et al.* Glioma cancer stem cells induce immunosuppressive macrophages/microglia. *Neuro Oncol* 2010; **12**: 1113 25.
38 Kubota Y, Takubo K, Shimizu T *et al.* M-CSF inhibition selectively targets pathological angiogenesis and lymphangiogenesis. *J Exp Med* 2009; **206**: 1089 102.
39 Priceman SJ, Sung JL, Shaposhnik Z *et al.* Targeting distinct tumor-infiltrating myeloid cells by inhibiting CSF-1 receptor: combating tumor evasion of antiangiogenic therapy. *Blood* 2010; **115**: 1461 71.
40 Coniglio SJ, Eugenin E, Dobrenis K *et al.* Microglial stimulation of glioblastoma invasion involves EGFR and CSF-1R signaling. *Mol Med* 2012; **18**: 519 27.

doi: 10.1111/cas.12015

International Journal of
Radiation Oncology
biology • physics

www.redjournal.org

Clinical Investigation: Central Nervous System Tumor

Delayed Complications in Patients Surviving at Least 3 Years After Stereotactic Radiosurgery for Brain Metastases

Masaaki Yamamoto, MD,*,† Takuya Kawabe, MD,*,‡ Yoshinori Higuchi, MD,§ Yasunori Sato, PhD,|| Tadashi Nariai, MD,¶ Bierta E. Barfod, MD,* Hidetoshi Kasuya, MD,† and Yoichi Urakawa, MD*

**Katsuta Hospital Mito GammaHouse, Hitachi-naka; †Department of Neurosurgery, Tokyo Women's Medical University Medical Center East, Tokyo; ‡Department of Neurosurgery, Kyoto Prefectural University of Medicine Graduate School of Medical Sciences, Kyoto; §Department of Neurosurgery and ||Clinical Research Center, Chiba University Graduate School of Medicine, Chiba; and ¶Department of Neurosurgery, Graduate School, Tokyo Medical and Dental University School of Medicine, Tokyo, Japan*

Received Mar 16, 2012, and in revised form Apr 5, 2012. Accepted for publication Apr 6, 2012

Summary

This retrospective investigation analyzed delayed complications in patients with brain metastases treated with stereotactic radiosurgery (SRS). Among 167 brain metastasis patients surviving more than 3 years after SRS, 17 (10.2%) experienced delayed complications occurring 24.0-121.0 months (median, 57.5 months) after SRS. The actuarial incidences of delayed complications estimated by competing risk analysis were 4.2% at the 60th month and 21.2% at the 120th month after SRS. Among various clinical

Purpose: Little is known about delayed complications after stereotactic radiosurgery in long-surviving patients with brain metastases. We studied the actual incidence and predictors of delayed complications.

Patients and Methods: This was an institutional review board-approved, retrospective cohort study that used our database. Among our consecutive series of 2000 patients with brain metastases who underwent Gamma Knife radiosurgery (GKRS) from 1991-2008, 167 patients (8.4%, 89 women, 78 men, mean age 62 years [range, 19-88 years]) who survived at least 3 years after GKRS were studied.

Results: Among the 167 patients, 17 (10.2%, 18 lesions) experienced delayed complications (mass lesions with or without cyst in 8, cyst alone in 8, edema in 2) occurring 24.0-121.0 months (median, 57.5 months) after GKRS. The actuarial incidences of delayed complications estimated by competing risk analysis were 4.2% and 21.2% at the 60th month and 120th month, respectively, after GKRS. Among various pre-GKRS clinical factors, univariate analysis demonstrated tumor volume-related factors: largest tumor volume (hazard ratio [HR], 1.091; 95% confidence interval [CI], 1.018-1.154; $P=.0174$) and tumor volume ≤ 10 cc vs >10 cc (HR, 4.343; 95% CI, 1.444-12.14; $P=.0108$) to be the only significant predictors of delayed complications. Univariate analysis revealed no correlations between delayed complications and radiosurgical parameters (ie, radiosurgical doses, conformity and gradient indexes, and brain volumes receiving >5 Gy and >12 Gy). After GKRS, an area of prolonged enhancement at the irradiated lesion was shown to be a possible risk factor for the development of delayed complications (HR, 8.751; 95% CI, 1.785-157.9; $P=.0037$). Neurosurgical interventions were performed in 13 patients (14 lesions) and mass removal for 6 lesions and Ommaya reservoir placement for the other 8. The results were favorable.

Reprint requests to: Masaaki Yamamoto, MD, Katsuta Hospital Mito GammaHouse, 5125-2 Nakane, Hitachi-naka, Ibaraki 312-0011 Japan. Tel: (+81) 29-271-0011; Fax: (+81) 29-274-1475; E-mail: BCD06275@nifty.com

Conflict of interest: none.

Int J Radiation Oncol Biol Phys, Vol. 85, No. 1, pp. 53–60, 2013
0360-3016/$ - see front matter
doi:10.1016/j.ijrobp.2012.04.018

factors before SRS, the only significant predictors of delayed complications were volume-related factors.

Conclusions: Long-term follow-up is crucial for patients with brain metastases treated with GKRS because the risk of complications long after treatment is not insignificant. However, even when delayed complications occur, favorable outcomes can be expected with timely neurosurgical intervention. © 2013 Elsevier Inc.

Introduction

Brain metastases, a common neurologic problem, are life-threatening for cancer patients in the absence of effective treatment. Recently, stereotactic radiosurgery (SRS) has become an established treatment option for brain metastases (1). SRS is more advantageous than other treatment options (ie, whole brain radiation therapy [WBRT], surgery, systemic anticancer agents, and combinations of these modalities) in terms of costs, hospitalization, morbidity, mortality, and wider applicability and repeatability (2). Although numerous prospective or retrospective series, as extensively reviewed by McDermott and Sneed (2), have reported the results of local control, survival, and/or complications in patients with brain metastases treated by SRS, little is known about delayed complications in long-surviving patients with brain metastases after SRS. We previously reported 8 patients with brain metastases and delayed cyst formation detected by magnetic resonance imaging (MRI) more than 3 years after Gamma Knife radiosurgery (GKRS) (3). Herein, we present post-GKRS delayed complications, including those of the cases described in our prior publication, and we clarify the actual incidence, clinical factors, and radiosurgical parameters predicting delayed complications. In this study, delayed complications were defined as Radiation Therapy Oncology Group (RTOG) neurotoxicity grade 2 or worse occurring more than 2 years after GKRS (4). Also, even patients with grade 0 delayed complications were included if neurosurgical intervention was required. Furthermore, we discuss the treatment and pathogenesis of these complications based on histopathologic studies.

Methods and Materials

Patient population

This was an institutional review board (IRB)-approved, retrospective cohort study using our database (IRB #1981). Among our consecutive series of 2000 patients with brain metastases who underwent GKRS between July 1991 and June 2008, 167 (8.4%) who survived for at least 3 years after GKRS were studied. Table 1 summarizes their clinical characteristics. The patients in our series underwent GKRS alone, without WBRT, for newly diagnosed or recurrent brain metastases after WBRT or surgery. In our facility, all patients had been referred to us for GKRS by their primary physicians. Therefore, patient selection had mostly been made outside of our facilities. The patient selection criteria may well have differed somewhat among the referring physicians. Therefore, the first author (M.Y.) ultimately decided whether or not a patient would be accepted for GKRS in all cases. Therefore, as shown in Table 1, only 1 patient was categorized into recursive partitioning analysis class 3 (5).

The treatment strategy was explained in detail to each patient and at least 1 of their adult relatives by the first author (M.Y.), and written informed consent was obtained from all patients before GKRS. Standard, single-session GKRS was performed. The selected tumor periphery doses ranged from 10.0 Gy-25.0 Gy (median, 24.0 Gy). Excluding 1 deceased patient (patient 8), the remaining 5 agreed to the use of their histopathologic photographs for this publication.

Discriminating local recurrence from delayed complications

The criteria for local recurrence (recurrence of the GKRS-irradiated lesion) were usually an increase in the size of the enhanced area on postgadolinium T1-weighted MRI, an enlarged tumor core on T2-weighted MR images, and the detection of a high choline peak on proton MR spectrograms. However, in some cases in which MRI raised a suspicion of recurrence, methionine positron emission tomography (PET) was used for determining whether or not the tumor had recurred. These PET examinations were performed and the results were evaluated by 1 of the authors (TN) who was not involved in either GKRS treatment or patient follow-up.

Statistical analysis

All data were analyzed according to the intention-to-treat principle. For baseline variables, summary statistics were constructed that used frequencies and proportions for categoric data, means, and standard deviations for continuous variables. We compared patient characteristics using Fisher's exact test for categorical outcomes and t tests for continuous variables, as appropriate.

For time-to-event outcomes, the cumulative incidence of delayed complications was estimated by a competing risk analysis, because death is a competing risk for loss to follow-up (ie, patients who die can no longer become lost to follow-up) (6). Also, to identify the baseline and clinical variables associated with delayed complications, univariate competing risk analysis was performed with the Fine-Gray generalization of the proportional hazards model, which accounts for death as a competing risk (7).

All comparisons were planned, and the tests were 2-sided. A P value less than .05 was considered to indicate a statistically significant difference. One of the authors (Y.H.) initially cleaned and finalized the database using JMP, Japanese version 9.0 for the Windows system (SAS Institute, Inc., Cary, NC). Thereafter, the other author (Y.S.) independently performed statistical analyses using the SAS software program, version 9.2 (SAS Institute, Inc.) and the R statistical program, version 2.13. These 2 authors were not involved in either GKRS treatment or patient follow-up.

Results

Overall survival and salvage treatment

The overall median survival time after GKRS was 7.3 months (95% confidence interval [CI], 6.9-7.8 months) in our cohort of

Table 1 Clinical characteristics of brain metastasis patients

Categories	Overall	Complication(s) (+)	Complication(s) (−)	*P* values*
No. of patients	167	17	150	
Mean age (y)	62	60	62	.3855
Range	19-88	35-71	19-88	
Sex				
Female	89	9 (53%)	80 (53%)	1.000
Male	78	8	70	
Primary cancer				
Lung	101	12 (71%)	89 (59%)	.4405
Nonlung	66	5	61	
Primary cancer, Controlled	124	15 (88%)	109 (73%)	.2432
Extracranial METs, No	118	13 (76%)	105 (70%)	.7801
KPS				
≥80%	160	16 (94%)	144 (96%)	.5352
≤70%	7	1	6	
RPA class				
I	49	8	41	
II	117	9 (53%)	108 (72%)	.1593†
III	1	0	1	
Neurologic symptoms	97	11 (65%)	86 (57%)	.6439
Prior surgery	45	3 (18%)	42 (28%)	.5645
Prior WBRT	4	1 (6%)	3 (2%)	.3342
Tumor numbers				
Mean	3	4	3	.4599
Range	1-36	1-29	1-36	
Solitary	91	9 (53%)	82 (55%)	1.000
Tumor volume (cc)‡				
Mean	4.13	7.03	3.80	.0152
Range	0.02-30.30	0.35-20.60	0.02-30.30	
≤10 cc	145	11	134	
>10 cc	22	6 (35%)	16 (11%)	.0124
Peripheral dose (Gy)				
Mean	22.0	21.4	22.1	.3209
Range	10.0-25.0	15.0-25.0	10.0-25.0	
Tumor nature				
Solid	125	14	112	
Cystic	42	3 (18%)	39 (25%)	.7663
Peritumoral edema	58	7 (42%)	51 (34%)	.5960
Accompanying hemorrhage	12	0	12 (8%)	.6139
Prolonged enhanced area§	93	16 (94%)	77 (57%)	.0028

Abbreviations: KPS = Karnofsky performance status; RPA = recursive partitioning analysis; WBRT = whole brain radiation therapy.

* Student's *t* test was used for continuous variables and Fisher's exact test for pairs of categoric variables.

† RPA class II vs classes I and III.

‡ Tumors causing delayed complications in the complication (+) group and the largest tumors in the complication (−) group.

§ Demonstrated on magnetic resonance imaging (MRI) performed at the 12th post-treatment month or later (16 patients were excluded because MRI results were not available).

2000 patients. In the subset reported herein, the median post-GKRS follow-up time among censored observations was 49.9 months (range, 36.0-142.0 months), and 92 patients (55.1%) had died as of the end of July 2011. The median survival time after GKRS was 61.8 months (95% CI, 56.3-68.4 months). The actuarial post-GKRS survival rates were 52.7% at 60 months and 28.0% at 120 months after GKRS. The causes of death could not be determined in 4 patients but were confirmed in the remaining 88 to be nonbrain diseases in 72 (81.8%) and brain diseases in 16 (18.2%). Although no further salvage GKRS was required in 68 patients (40.7%), 99 (59.3%) underwent salvage GKRS mostly for newly developed lesions and/or, rarely, recurrence of the treated lesions: twice in 47 patients, 3 times in 24, 4 times in 13, and 5 times or more in 15 (maximum, 8 times). Four patients also underwent surgical removal because of recurrence of the irradiated lesion, and 5 received WBRT for meningeal dissemination.

Incidence and treatment of delayed complications

Among these 167 patients, 17 (10.2%) experienced delayed complications occurring 24-121 months (median, 53 months) after

Table 2 Patients with delayed complications

Patient	Age/sex	Origin	Tumor, no/vol (cc)	Dose (Gy), min/max	RTOG grade	MRI findings	Onset (mo after GKRS)	Treatment	Post-GKRS salvage
1*	63/F	Lung (ad)	1/9.2	15.0/30.0	4	Edema	40	Medical treatment	None
2	66/F	Lung (ad)	1/2.3	25.0/29.4	3	Mass with cyst	121	Op recommended, but refused	None
3	70/F	Breast	1/6.2	20.0/40.0	0	Mass with cyst (left) cyst (right)	48	Removal ORP	GKRS
4	58/M	Lung (ad)	2/1.6	25.0/50.0	2	Cyst	48	ORP	GKRS
5	70/F	Lung (ad)	2/19.6	20.0/40.0	4	Mass with cyst	60	Op recommended, but refused	GKRS
6	66/M	Lung (scc)	1/0.6	22.0/44.0	2	Mass with cyst	105	Removal	GKRS
7	63/F	Ovary	4/11.3	20.0/33.3	0	Cyst	58	ORP	GKRS
8	71/M	Lung (ad)	1/0.4	25.0/27.8	3	Mass	44	Removal	None
9	42/M	Kidney	1/2.0	24.0/40.0	3	Cyst	71	ORP	GKRS
10	69/F	Lung (ad)	10/3.2	20.0/33.3	4	Edema	52	Medical treatment	GKRS
11	63/F	Lung (ad)	4/1.2	25.0/50.0	0	Mass with cyst	112	Removal	None
12	55/M	Lung (sq)	2/5.0	20.0/40.0	0	Cyst	105	ORP	None
13	59/F	Lung (ad)	2/10.9	21.0/35.0	0	Mass with cyst	102	Removal	None
14	35/M	Lung (ad)	1/11.1	21.0/35.0	2	Mass	27	Removal	None
15	54/M	Lung (ad)	4/3.2	24.0/40.0	0	Cyst	53	ORP	GKRS
16	46/F	Breast	29/20.6	15.0/30.0	3	Cyst	24	ORP	GKRS
17	62/M	Pharynx	1/13.1	21.0/35.0	0	Cyst	50	ORP	None

Abbreviations: ad = adenocarcinoma; GKRS = Gamma Knife radiosurgery; max = maximum; min = minimum; mo = months; MRI = magnetic resonance imaging; Op = operation; ORP = Ommaya reservoir placement; scc = small cell carcinoma; sq = squamous cell carcinoma; vol = volume.
* This patient had undergone whole brain radiation therapy before GKRS.

GKRS, as shown in Table 2. In the 17 patients, although no further salvage GKRS was required in 8 patients, 9 underwent salvage GKRS. In 1 patient (patient 3), cyst formation occurred in the areas of 2 lesions, 1 with a mass on the left side and the other with no masses. Among a total of 18 lesions, mass lesions occurred in 6, 6 with and 2 without associated cyst, a simple cyst in 8, and extensive edema in the other 2. As shown in Fig. 1, the actuarial incidences of delayed complications estimated with competing risk analysis were 4.2% and 21.2% at the 60th month and 120th month, respectively, after GKRS. Although, as described below,

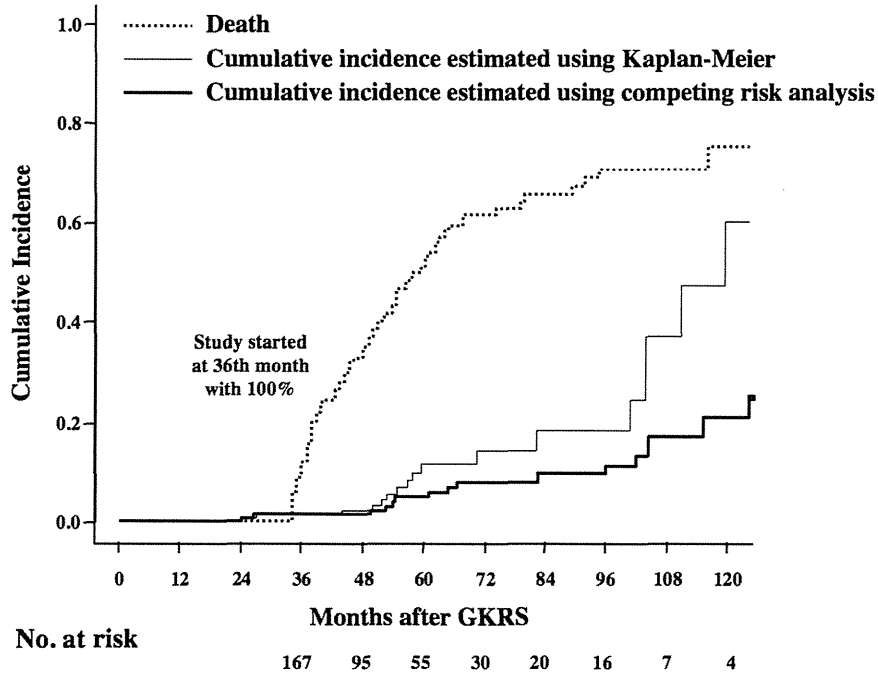

Fig. 1. Cumulative incidence of delayed complications after Gamma Knife radiosurgery (GKRS) estimated by the Kaplan-Meier method vs competing risk analysis.

7 patients were asymptomatic, the other 10 experienced various neurologic symptoms; 3 with RTOG neurotoxicity grade 2, 4 with grade 3, and 3 with grade 4 (4).

One patient (patient 1) who had undergone WBRT with a total dose of 50 Gy before GKRS experienced a progressive decrease in neurocognitive function (NCF). Although this patient was treated medically, NCF progressively deteriorated, and she ultimately died because of malnutrition-induced emaciation, as previously reported in detail including autopsy findings (8). Another patient (patient 10) experienced severe steroid-refractory edema. Expanding mass lesions with cyst formation were demonstrated by sequential MRI studies in 2 patients (patients 2 and 5). Although we strongly recommended surgical intervention for these patients, both refused and received only medical treatment. Their symptoms showed no amelioration. In the 12 remaining patients (13 lesions), neurosurgical intervention was performed: mass removal for 6 lesions and Ommaya reservoir placement for the other 8. Among these 12 patients, 6 with neurologic symptoms experienced complete recovery. Although no neurologic symptoms had developed, surgical intervention was performed for the other 7 because sequential MRI follow-up had demonstrated progressive enlargement of a cyst and/or a mass lesion, and further observation had thus been regarded as constituting an excessively high risk. During the median postsurgical interval of 25 months (range, 2-80 months), the 12 patients experienced no further exacerbation until death or the latest follow-up day. Among 8 patients who had undergone Ommaya reservoir placement, repeated aspiration with a 1-3-month interval was required in 2, and no further aspiration was necessary in the other 6.

Factors affecting delayed complications

As shown in Tables 1 and 3, among various pre-GKRS clinical factors, univariate analysis demonstrated tumor volume-related factors: largest tumor volume (HR, 1.091; 95% CI, 1.018-1.154; $P=.0174$) and tumor volume $\leq$10 cc vs >10 cc (HR, 4.343; 95% CI, 1.444-12.14; $P=.0108$) to be the only significant predictors of delayed complications. Univariate analysis revealed no correlations between delayed complications and radiosurgical parameters (ie, radiosurgical doses, conformity and gradient indexes, and brain volumes receiving >5 Gy and >12 Gy) (9-12). After GKRS, an area of prolonged enhancement at the irradiated lesion on MRI performed at the 12th post-treatment month or later was shown to be a possible risk factor for delayed complications (HR, 8.751; 95% CI, 1.785-157.9; $P=.0037$).

Neuroimaging and pathology

Among the 17 patients who experienced delayed complications, a progressively expanding mass lesion developed in 8. Sequential MRI studies, methionine PET scans or proton MR spectrograms, and histologic findings in these 8 patients are shown in Figs. 2 and 3. Histologic examinations were not available in 2 patients (patients 2 and 5) because they refused surgery. However, high methionine uptake was not demonstrated on PET scans in patient 2, and a higher choline peak was not seen on the proton MR spectrogram in patient 5. Therefore, we considered recurrence to be unlikely in these mass lesions. Histologic studies were performed in the other 6 patients, and no tumor cells were found. Characteristic histologic features were hypocellular scar tissue consisting of fibrous tissue with degenerative cells, sinusoid formation, variously sized vessels, endothelial proliferation, various stages of hemorrhage, and hemosiderin deposits.

Table 3 Clinical factors affecting incidence of delayed complications (167 patients)

Clinical factors	Univariate analysis HR	95% CI	*P* values
Age			
Continuous	1.010	0.977-1.051	.5730
<65 vs ≥65 y	0.949	0.324-2.523	.9192
Sex: female vs male	1.073	0.402-2.812	.8851
KPS: ≥80% vs ≤70%	5.192	0.278-28.52	.2067
Primary cancer: lung vs nonlung	0.398	0.124-1.098	.0761
Prior surgery: no vs yes	0.474	0.109-1.457	.2072
Prior WBRT: no vs yes	0.908	0.049-4.797	.9265
GKRS procedures			
Continuous	1.153	0.820-1.524	.3830
Single vs multiple	1.155	0.424-3.225	.7775
Tumor numbers			
Continuous	1.066	0.968-1.131	.1567
Solitary vs multiple	0.699	0.266-1.841	.4710
Tumor volume			
Cumulative	1.090	1.022-1.151	.0117
Largest tumor*	1.091	1.018-1.154	.0174
≤10 cc vs >10 cc	4.343	1.444-12.14	.0108
Tumor nature			
Solid vs cystic	1.057	0.335-4.644	.9313
Peritumoral edema: yes vs no	1.589	0.574-4.167	.3586
Accompanying hemorrhage: yes vs no	NA	NA	.1783
Area of prolonged enhancement: yes vs no†	8.751	1.785-157.9	.0037
Dose			
Minimum	1.008	0.905-1.147	.8977
Maximum	1.025	0.961-1.096	.4517
Conformity index‡	10.33	0.355-378.4	.1765
Gradient index‡	1.427	0.601-3.125	.4186
Brain volume receiving >5 Gy‡	1.000	0.994-1.003	.8558
Brain volume receiving >12 Gy‡	1.005	0.983-1.021	.5915

Abbreviations: CI = confidence interval; GKRS = Gamma Knife radiosurgery; HR = hazard ratio; KPS = Karnofsky performance status; NA = not available; WBRT = whole brain radiation therapy.

* Tumors causing delayed complications in the complication (+) group and the largest tumors in the complication (-) group.

† Demonstrated on magnetic resonance imaging (MRI) performed at the 12th post-treatment month or later (16 patients were excluded because MRI results were not available).

‡ Based on 162 patients (5 were excluded because treatment data were lost owing to technical problems).

Discussion

Historically, the purpose of treating patients with brain metastases has been symptom palliation and maintenance of good condition during the patient's relatively short remaining life expectancy.

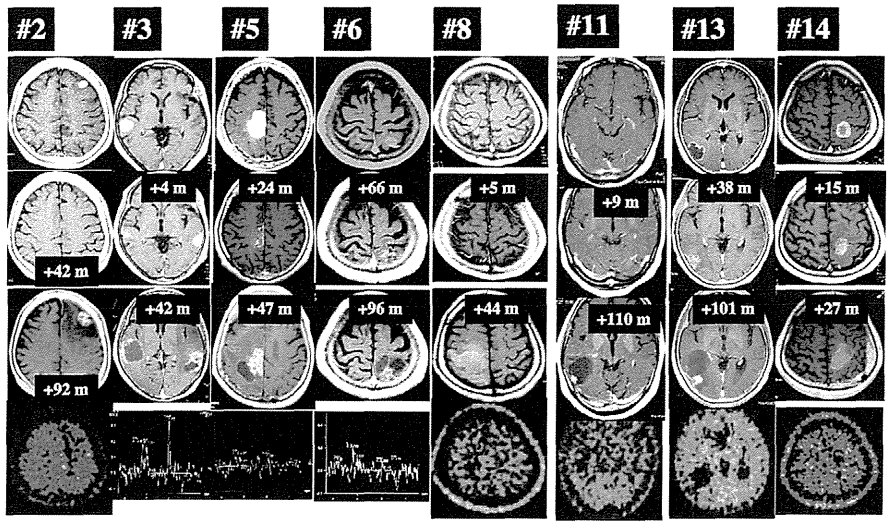

Fig. 2. Sequential magnetic resonance (MR) images, methionine positron emission tomographic (PET) scans, or proton MR spectrograms of 8 patients. Patient numbers are shown above each column. MRI was performed at the time of Gamma Knife radiosurgery (GKRS) (*top row*), at the time of confirmed tumor control (at the time of the second GKRS for a left temporal tumor in patient 3) (*second row*), and at the time of the development of delayed complications (*third row*). Methionine PET scans or proton MR spectrograms were obtained at nearly the same times as the upper MR examinations (*bottom row*).

Therefore, treatment-related complications occurring with a long latency period have seldom been a matter of primary concern. However, SRS, which is a less invasive procedure and allows long-term tumor control, has recently become a common treatment for brain metastases (1, 2). As we have reported elsewhere, GKRS was shown to benefit patients by decreasing the likelihood of death from neurologic causes (approximately 10%) (8, 13). The widespread use of SRS for patients with brain metastases has recently prompted physicians to continue, rather than give up, as in the former era, aggressive treatment of original tumors and/or extracranial metastases. With recent advances in cancer treatment, considerable numbers of patients can survive for many years after the initial diagnosis. This has raised concern regarding post-SRS complications occurring with a prolonged latency period. Very recently, learning how to avoid and treat these complications has been seen as crucial. To the best of our knowledge, this retrospective investigation is the first to analyze the long-term toxicity of SRS in patients surviving at least 3 years after treatment of brain metastases.

Incidences of complications

Williams et al (14) recently reported the incidences of post-SRS complications and their predictive factors based on a comprehensive review of 273 patients (316 treated lesions) undergoing SRS for 1 or 2 brain metastases. According to their investigation, complications, mostly seizure onset, were associated with 127 (40%) of 316 treated lesions. Severe complications were more likely to occur more than 30 days after SRS. Progression of the

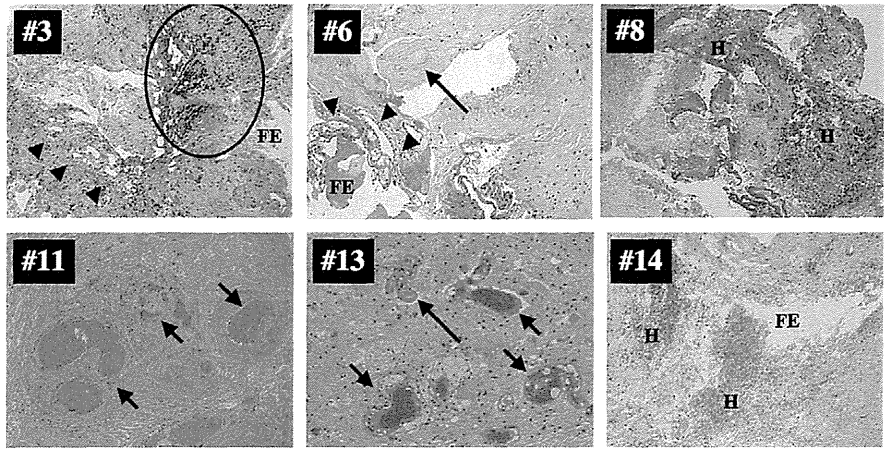

Fig. 3. Histopathologic findings in 6 patients. Excluding 1 deceased patient (patient 8), the remaining 5 agreed to the use of their histopathologic photographs for this publication. Patient numbers are shown in each image. Notice variously sized vessels (*short arrows*), endothelial proliferation (*long arrows*), sinusoid formation (*arrowhead*), fluid exudation (*FE*), various stages of hemorrhage (*H*), and hemosiderin deposits (*circle*). (Hematoxylin and eosin, original magnifications not available.)

primary cancer and tumor location in the eloquent cortex were significantly associated with complications. However, no chronologic data were presented in their article, and there was no description of delayed complications. Varlotto et al reported (11) that among 137 patients with brain metastases who survived for at least 1 year after GKRS, postradiosurgical sequelae developed in 2.8% and 11.4% of patients at the first and fifth year, respectively, after GKRS. The incidence of 11.4% at the fifth post-GKRS year was far higher than our result, 4.2%. In their study, only the standard Kaplan-Meier method was used. This method assumes that follow-up of those developing a competing event (death) is simply censored. We consider competing risk analysis to have been necessary for evaluation of their data (6, 7). Furthermore, their Kaplan-Meier plot of the proportion without neurologic sequelae showed that none of their patients experienced neurologic sequelae between the 24th and 120th post-GKRS months. In other words, Varlotto et al (11) observed complications that occurred in a somewhat earlier post-GKRS period, 2 years or less. By contrast, herein we have described delayed complications occurring 24 months or more after GKRS, and our data demonstrated a time-related increase in the incidence (Fig. 1).

Predictive factors

Several authors have shown correlations with tumor volume and/or WBRT and complications (11, 14-17). In our present study, the only factor associated with delayed complications was larger tumor volume. Nakagawa et al reported prior or concomitant WBRT to be a possible risk factor for low-grade dementia (16). We also observed 1 patient in whom severe dementia occurred after WBTR followed by GKRS (8). However, in our series, a small number of patients—only 4—underwent WBRT, so the correlation between WBRT and delayed complications was unclear. It is common knowledge in radiobiology that higher irradiation doses carry a higher risk of complications. The median peripheral dose, 24.0 Gy, in the subset reported here was higher than the 21.0 Gy in our entire cohort (2000 cases). We cannot deny that such a relatively high dose may have an impact on delayed complications, although univariate analysis did not demonstrate the peripheral dose to be a predictive factor for delayed complications in this study (Table 3).

Paddick and Lippitz (10) found, among several radiosurgical parameters, the gradient index to be a crucial factor for complication avoidance. Also, Ishikawa et al (3) described, as noted in our previous report on delayed cyst formation after GKRS for patients with brain metastases, that a poor gradient index may partially explain the observed phenomenon. However, univariate analysis did not demonstrate the gradient index to be a predictive factor for delayed complications in this study. Although Varlotto et al (11) found that complications correlated with brain volume receiving $\geq$12 Gy and we reported receiving $\geq$5 Gy to be important (12), neither $\geq$12 Gy nor $\geq$5 Gy irradiated brain volume was associated with delayed complications in our present study.

Pathogenesis

The first author (M.Y.) previously reported post-GKRS sequelae (ie, expanding mass lesions with or without cyst formation) occurring many years after GKRS for arteriovenous malformations (18, 19). Our present study revealed similar complications to occur in long-term survivors after GKRS for brain metastases. As noted in our previous report, the mechanism of delayed cyst formation after GKRS for brain metastases is speculated to be increased permeability through partially injured blood vessel walls within the degenerated or scar tissue (3). However, the mechanism of enhanced mass lesions has yet to be fully elucidated. The histopathologic changes of resected specimens in the 6 cases reported herein were characterized as degenerated tissue mainly consisting of fibrous tissue and various stages of hemorrhage, from fresh to organized with hemosiderin deposits. Also, there was evidence of neovascularization, enlarged vessels, and albuminous fluid exudation. In most cases, the irradiated metastatic lesions showed findings from coagulation necrosis to liquefaction necrosis and ultimately collapsed, as Szeifert et al very recently described (20). However, we speculate that in some other cases, degenerated tissue remains for many years and reparative processes may occur after repeated intranidal microhemorrhage, which may finally cause an expanding mass lesion, although the triggering mechanism remains unknown. Therefore, the existence of a long-standing enhanced area may be a risk factor for delayed complications.

Treatment

Observation alone is reasonable for compensated and asymptomatic patients because spontaneous regression can be expected in some, as is the case in patients with arteriovenous malformations. When delayed cysts and/or enhanced mass lesions are symptomatic, surgical intervention should be considered. Even if these conditions have not yet produced neurologic symptoms, surgical intervention is recommended for patients whose cysts and/or mass lesions show continuous expansion. For a patient with a simple cyst, we believe that Ommaya reservoir placement may be a better choice than fluid aspiration without a reservoir, because some patients require reaspiration. Moreover, Ommaya tube placement may maintain the drainage tract from the cyst to the subarachnoid space, thereby preventing cyst regrowth. For a patient with an enhanced mass lesion with or without cyst formation, however, surgical resection should be considered even if the mass lesion is not particularly large. In any case, the surgical results of our present series were favorable.

Conclusions

In conclusion, 10.2% of long-surviving patients showed delayed complications, with a median interval of 53 months (range, 24.0-121.0 months) after GKRS for brain metastases. A larger tumor volume, particularly larger than 10 cc, was a risk factor for these complications. Long-term follow-up is crucial for patients with brain metastases treated with GKRS because the risk of complications long after treatment is not insignificant. However, if a delayed complication does occur, a favorable outcome can be expected with timely surgical intervention. This is considered to be quite different from WBRT, which causes the untreatable complication of decreased NCF.

References

1. Linskey ME, Andrews DW, Asher AL, et al. The role of stereotactic radiosurgery in the management of patients with newly diagnosed brain metastases: a systematic review and evidence-based clinical practice guideline. *J Neurooncol* 2010;96:45-68.

2. McDermott MW, Sneed PK. Radiosurgery in metastatic brain cancer. *Neurosurgery* 2005;57(Suppl S4):45-53.
3. Ishikawa E, Yamamoto M, Saito A, et al. Delayed cyst formation after gamma knife radiosurgery for brain metastases. *Neurosurgery* 2009; 65:689-695.
4. Radiation Therapy Oncology Group Cooperative Group Common Toxicity Criteria. http://www.rtog.org/ResearchAssociates/AdverseEvent Reporting.aspx. Accessed September 30, 2011.
5. Gasper L, Scott C, Rotman M, et al. Recursive partitioning analysis (RPA) of prognostic factors in three Radiation Therapy Oncology Group (RTOG) brain metastases trials. *Int J Radiat Oncol Biol Phys* 1997;37:745-751.
6. Gooley TA, Leisenring W, Crowley J, et al. Estimation of failure probabilities in the presence of competing risks: new representations of old estimators. *Stat Med* 1999;18:695-706.
7. Fine JP, Gray RJ. A proportional hazards model for the subdistribution of a competing risk. *J Am Stat Assoc* 1999;94:496-509.
8. Yamamoto M. Radiosurgery for metastatic brain tumors. *Prog Neurol Surg* 2007;20:106-128.
9. Paddick I. A simple scoring ratio to index the conformity of radiosurgical treatment plans. *J Neurosurg* 2000;93(Suppl):219-222.
10. Paddick I, Lippitz B. A simple dose gradient measurement tool to complement the conformity index. *J Neurosurg* 2006;105(Suppl): 194-201.
11. Varlotto JM, Flickinger JC, Niranjan A, et al. Analysis of tumor control and toxicity in patients who have survived at least one year after radiosurgery for brain metastases. *Int J Radiat Oncol Biol Phys* 2003;57:452-464.
12. Yamamoto M, Ide M, Nishio S, et al. Gamma knife radiosurgery for numerous brain metastases: is this a safe treatment? *Int J Radiat Oncol Biol Phys* 2002;53:1279-1283.
13. Yamamoto M, Kawabe T, Bierta E, et al. How many metastases can be treated with radiosurgery? *Prog Neurol Surg* 2012;26: 261-272.
14. Williams BJ, Suki D, Fox BD, et al. Stereotactic radiosurgery for metastatic brain tumors: a comprehensive review of complications. *J Neurosurg* 2009;111:439-448.
15. Joseph J, Adler JR, Cox RS, et al. Linear accelerator-based stereotaxic radiosurgery for brain metastases: the influence of number of lesions on survival. *J Clin Oncol* 1996;14:1085-1092.
16. Nakagawa K, Tago M, Terahara A, et al. A single institutional outcome analysis of gamma knife radiosurgery for single or multiple brain metastases. *Clin Neurol Neurosurg* 2000;102:227-232.
17. Shiau CY, Sneed PK, Shu H, et al. Radiosurgery for brain metastases: relationship of dose and pattern of enhancement to local control. *Int J Radiat Oncol Biol* 1997;37:375-383.
18. Yamamoto M, Jimbo M, Hara M, et al. Gamma knife radiosurgery for arteriovenous malformations: long-term follow-up results focusing on complications occurring more than five years after irradiation. *Neurosurgery* 1996;38:906-914.
19. Yamamoto M, Hara M, Ide M, et al. Radiation-related adverse effects observed on neuro-imaging several years after radiosurgery for cerebral arteriovenous malformations. *Surg Neurol* 1998;49: 387-398.
20. Szeifert GT, Kondziolka D, Lunsford LD, et al. The contribution of pathology to radiosurgery. *Prog Neurol Surg* 2007;20:1-15.

IDH1/2 mutation is a prognostic marker for survival and predicts response to chemotherapy for grade II gliomas concomitantly treated with radiation therapy

YOSHIKO OKITA[1], YOSHITAKA NARITA[1], YASUJI MIYAKITA[1], MAKOTO OHNO[1], YUKO MATSUSHITA[1], SHINTARO FUKUSHIMA[2], MINAKO SUMI[3], KOICHI ICHIMURA[4], TAKAMASA KAYAMA[1] and SOICHIRO SHIBUI[1]

Departments of [1]Neurosurgery and Neuro-Oncology, [2]Pathology and Clinical Laboratories and [3]Radiation Oncology, [4]Division of Brain Tumor Translational Research, National Cancer Center, Tokyo 104-0045, Japan

Received April 27, 2012; Accepted June 29, 2012

DOI: 10.3892/ijo.2012.1564

Abstract. Reliable prognostic biomarkers of grade II gliomas remain unclear. This study aimed to examine the role of mutations of isocitrate dehydrogenase (*IDH1/2*), 1p/19q co-deletion, and clinicopathological factors in patients with grade II glioma who were primarily treated with radiotherapy or chemoradiotherapy after surgery. Seventy-two consecutive patients, including 49 cases of diffuse astrocytomas (DA), 4 oligodendrogliomas (OL) and 19 oligoastrocytomas (OA), who underwent treatment from 1991 to 2010 at a single institution were examined. The overall survival (OS) of the DA patients (8.3 years) was significantly shorter than that of the OL and OA patients (11.7 years). *IDH1/2* mutations were found in 46.9% of the DA patients and 82.6% of the OL and OA patients. The progression-free survival (PFS) and OS of the patients with *IDH1/2* mutations (8.4 and 16.3 years) were significantly longer than those of the patients without *IDH1/2* mutations (3.3 and 4.5 years). Among the patients with *IDH1/2* mutations, those who were initially treated with chemoradiotherapy including nimustine hydrochloride (ACNU), had significantly longer PFS than those treated with radiotherapy alone, whereas no significant difference in PFS was observed between the chemo-radiotherapy and radiotherapy groups in the patients without *IDH1/2* mutations. Oligodendroglial tumors, age <40 years, initial Karnofsky performance status (KPS) ≥80, and *IDH1/2* mutations were favorable prognostic factors regarding PFS and OS. *IDH1/2* mutation was a predictive factor of response to chemoradiotherapy in grade II gliomas. Patients with *IDH1/2* mutations may benefit more from chemoraiotherapy than those without *IDH1/2* mutations.

Correspondence to: Dr Yoshitaka Narita, Department of Neuro-surgery and Neuro-Oncology, National Cancer Center Hospital, 5-1-1 Tsukiji, Chuo-ku, Tokyo 104-0045, Japan
E-mail: yonarita@ncc.go.jp

Key words: grade II gliomas, *isocitrate dehydrogenase 1*, *isocitrate dehydrogenase 2*, 1p/19q codeletion, chemoradiotherapy, diffuse astrocytoma

Introduction

World Health Organization (WHO) grade II gliomas (low-grade gliomas) are slow-growing tumors that include several subtypes, such as diffuse astrocytomas, mixed oligoastrocytomas, and oligodendrogliomas (1). The 10- and 20-year survival rates for patients with grade II glioma are reported to be 48 and 22% (2), reflecting the malignant potential of these tumors in long-term survival. Radiotherapy is often the treatment of choice for patients with incompletely resected grade II gliomas. However, the timing of radiotherapy for patients with these malignancies remains controversial and no difference in overall survival (OS) between groups receiving early and delayed radiation has been reported (3). Moreover, the efficacy of chemoradiotherapy for grade II gliomas is largely unknown. The addition of procarbazine, lomustine, and vincristine (PCV) therapy to radiotherapy for grade II gliomas conferred a significant increase in OS and progression-free survival (PFS) of >2 years in the Radiation Therapy Oncology Group (RTOG) 9802 study (4), suggesting that chemoradiotherapy might be effective for a subset of these patients.

Several studies have attempted to identify prognostic factors for grade II gliomas. To date, older age, astrocytic histology, the presence of neurologic deficits before surgery, larger tumor diameters, and tumors crossing the midline have been proposed as unfavorable prognostic factors (5-9). Several genetic markers, such as 1p/19q codeletion or mutations of the isocitrate dehydrogenase 1 and 2 genes (*IDH1/2*), have also been associated with patient survival. Oligodendrogliomas typically show 1p/19q codeletion (≤70%) (10,11), and its presence is reported to predict longer survival in oligodendroglial tumors (12). The 1p/19q codeletion is also a statistically significant predictor of prolonged survival in patients with astrocytomas (13). Furthermore, 1p/19q codeletion was associated with longer survival in all types of adult gliomas, independent of age and diagnosis (14,15). On the other hand, 1p/19q codeletion did not appear to be a sensitive prognostic biomarker in patients with either grade II astrocytic

or oligodendroglial tumors who did not receive radiotherapy or chemotherapy after surgery (16).

Mutations of the *IDH1/2* genes are common events in gliomas (17), especially among grade II gliomas, where *IDH1* mutations are observed in 70-80% of cases (11,17,18). Glioblastomas and anaplastic astrocytomas (WHO grade III) with IDH1/2 mutations have more favorable prognoses than those with a wild-type phenotype (17). Several studies have indicated that *IDH1/2* mutations are significantly associated with positive prognosis and chemosensitivity in low-grade gliomas (19,20), whereas others have reported that *IDH1/2* mutations were not associated with prognosis (21,22). Thus, the prognostic or predictive values of these genetic markers in grade II gliomas remain controversial.

In the present study, the clinicopathological factors, including age, Karnofsky performance status (KPS), histology, extent of resection, radiotherapy, chemoradiotherapy, largest tumor diameter, and MIB-1 staining index, as well as *IDH1/2* mutations and 1p/19q codeletion, were analyzed in grade II gliomas and correlated with the clinical course of the patients. Oligodendroglial tumors, age <40 years, initial KPS ≥80, and *IDH1/2* mutations were favorable prognostic factors for PFS and OS. The IDH1/2 mutation was a predictive factor of response to chemoradiotherapy in grade II gliomas.

Materials and methods

Patients and tissue collections. The data were collected from 72 patients who were found with WHO grade II gliomas at the first surgery. These included 49 diffuse astrocytomas and 23 oligodendroglial tumors, including 4 oligodendrogliomas and 19 oligoastrocytomas (male-female, 40:32; median age, 39.0 years). These consecutive cases were diagnosed and treated between 1991 and 2010 at the National Cancer Center Hospital in Japan. The clinical records of the patients were reviewed, and the data on the extent of tumor resection were obtained from the surgical report. Total or subtotal resection was defined as the removal of 90% or more of the tumor based on the surgeon's clinical report. Fifty-eight patients (80.6%) underwent initial surgeries followed by radiotherapy (22.2%) or chemoradiotherapy with ACNU (58.3%). Three patients with total or subtotal removal and 11 with partial resection or biopsy (19.4%) were followed-up without radiotherapy until progressive disease. Of the remaining patients, those who underwent initial treatment between 1991 and 2006 were treated with chemoradiotherapy and those treated between 2007 and 2010 underwent radiotherapy alone based on our treatment protocols. The radiation doses were 60 Gy before 2006 and 54 Gy after 2007. The chemotherapy in the diffuse astrocytoma cases consisted of ACNU administered twice during radiotherapy and 3 additional doses every 2 months after radiotherapy. The patients with oligodendroglial tumors received ACNU + VCR (vincristine) twice during radiotherapy, and thereafter, PAV [ACNU + VCR + PCZ (procarbazine)] was administered in 3 cycles every 2 months after radiotherapy. Each patient was worked up by MRI every 3-4 months until 2 years from the initial treatment and then every 6 months after 2 years. Progression was determined when the MRI showed a new enhancing lesion with Gd-DTPA, a new high intensity lesion or an obvious increased lesion (at least 20% larger than previous MRI in diameter) on T2/FLAIR images. Clinical deterioration of a patient was also determined as progression.

The formalin-fixed paraffin-embedded tumor samples and frozen specimens, when available, were collected from the primary resection for all the patients who underwent surgery in the National Cancer Center and whenever possible for those operated at other hospitals. The samples were examined for *IDH1/2* mutations and 1p/19q codeletion only when sufficient material for DNA extraction was available at either the primary or secondary resection. The study was approved by the internal review board of the National Cancer Center. The detailed information for all the 72 patients is listed in Table I.

Hematoxylin and eosin staining and immunohistochemical staining for MIB-1 and IDH1. The surgical specimens were fixed in 10% formalin and embedded in paraffin. The hematoxylin and eosin-stained specimens were examined to determine the histological tumor type. The multiple serial sections were subjected to immunohistochemical analyses (IHC) to visualize local staining. Antigen retrieval was carried out by exposing the tissue sections to 15 min of microwave heating in 0.1-mol/l sodium citrate (pH 6.0). This was followed with immunostaining of the specimens with the streptavidin-biotin-peroxidase complex method (Vectastain, Vector Laboratories, Inc., Burlingame, CA, USA). The samples were incubated in human monoclonal antibodies against MIB-1 (Dako, Tokyo, Japan). Positive immunostaining results were detected with the diaminobenzidine reaction, and the slides were subsequently counterstained with hematoxylin, dehydrated, cleared, and mounted.

Cell counting was performed with the aid of a light microscope (Olympus Corp., Tokyo, Japan). Cell counting was done at a magnification of x400. At least 200 tumor cells were counted, and the results were expressed as the mean of the counts obtained from 3 different locations within each specimen. The MIB-1-stained cells were also counted, and the percentage of the MIB-1-stained cells was calculated within the observed field and expressed as the MIB-1 index.

Human monoclonal antibodies specific against IDH1-R132H and IDH1-R132S were used to identify these 2 types of IDH1 mutations (Medical & Biological Laboratories, Tokyo, Japan). Positive immunostaining results were detected with the diaminobenzidine reaction, and the slides were subsequently counterstained with hematoxylin, dehydrated, cleared, and mounted. The positive granular cytoplasmic staining of the tumor cells was evaluated for mutant *IDH1* (23).

Extraction of nucleic acids. The tumor samples were immediately frozen in liquid nitrogen and stored at -80˚C. A peripheral blood sample was drawn from each patient and stored at -80˚C. Total DNA was extracted from either frozen tissue samples or paraffin-embedded specimens and from the patients' blood with a DNeasy Blood & Tissue kit (Qiagen Sciences, Germantown, MD, USA) according to the manufacturer's instructions.

Sequencing of IDH1/2. A 129-base pair (bp) fragment of *IDH1* containing codon 132 or a 150-bp fragment of *IDH2* containing codon 172 was PCR amplified using the forward primer IDH1f (CGGTCTTCAGAGAAGCCATT) and reverse primer IDH1r (GCAAAATCACATTATTGCCAAC) for *IDH1* and the forward primer IDH2f (AGCCCATCATCTGCAAAAAC) and

reverse primer IDH2r (CTAGGCGAGGAGCTCCAGT) for *IDH2* (18). The thermocycling conditions consisted of 5 min at 95°C, 35 cycles for 30 sec at 95°C, 40 sec at 56°C, and 50 sec at 72°C, followed by 10 min at 72°C. For confirmation, the forward primer IDH1fc (ACCAAATGGCACCATACGA) and reverse primer IDH1rc (TTCATACCTTGCTTAATGGGTGT) generating a 254-bp fragment and the forward primer IDH2fc (GCTGCAGTGGGACCACTATT) and reverse primer IDH2rc (TGTGGCCTTGTACTGCAGAG) generating a 293-bp fragment were used for amplification with the same thermocycling conditions (24). After the purification of the PCR products using the QIAquick PCR Purification kit (Qiagen), DNA sequencing for the *IDH1/2* gene was performed with an ABI PRISM 310 Genetic Analyzer (Applied Biosystems), using the same primers as for PCR.

1p and 19q status by fluorescence in situ hybridization. For fluorescence *in situ* hybridization (FISH), the tumor sections were deparaffinized in Hemo-De (Falma, Tokyo, Japan), dehydrated with 100% ethanol, and digested using a Paraffin Pretreatment kit (Vysis-Abbott, Tokyo, Japan) according to the manufacturer's protocol. Each section was hybridized with LSI 1p36/1q25 and LSI 19q13/19p13 probes (Vysis-Abbott). The probes and target DNA were denatured individually at 72°C for 5 min, followed by 2 overnight incubations at 37°C. Posthybridization washes were carried out in standard saline solution twice, and the sections were air-dried. The nuclei were counterstained with 4,6-diamidino-2-phenylindole. The sections were analyzed using a fluorescence microscope (Biorevo BZ-9000, Keyence, Japan).

The 1p or 19q deletions were considered present when the population of the cells with single 1p36 or single 19q13 was <50% of the cells with double 1p36 or double 19p13, respectively. At least 100 non-overlapping nuclei were counted per hybridization.

1p and 19q status by multiplex ligation-dependent probe amplification analysis. We used the SALSA P088 kit (MRC Amsterdam, The Netherlands) containing 16 1p probes (6 probe at 1p36), 8 19q probes, and 21 control probes specific to other chromosomes, including 2 probes for 19p. Information regarding the probe sequences and ligation sites can be found at http://www.mlpa.com. Multiplex ligation-dependent probe amplification (MLPA) analysis was performed as described previously (25,26). The 1p36 or 19q deletions were considered present when 5 of 6 markers for 1p36 and 5 of 8 markers for 19q in each chromosome arm had normalized ratios <0.75.

Statistical analysis. All the statistical analyses, including the Kaplan-Meier survival analysis, were performed using the JMP ver. 8 software (Tokyo, Japan). The multivariate analysis with Cox regression, which was used to assess the independent prognostic factors for all the 72 cases, was performed only for the variables with $p<0.1$ and which included the data obtained in the univariate analysis for all the patients. A similar analysis was performed for 58 cases with radiotherapy or chemoradiotherapy.

Results

Progression-free and OS. The PFS and median OS times for all the 72 grade II glioma patients were 5.8 and 10.3 years, respectively (male-female, 40:32; median age, 39.0 years; Table I).

Table I. Characteristics of patients with grade II gliomas.

Characteristic	No. of patients	Years	Percentage (%)
Sex			
Male	40		55.6
Female	32		44.4
Age (years)			
Median		39	
Range		21-75	
Histology			
Astrocytoma	49		68
Oligodendroglioma	4		6
Oligoastrocytoma	19		26
Extent of removal			
Total removal	12		16.7
Subtotal removal	2		2.8
Partial removal	27		37.5
Biopsy	31		43.1
Largest diameter of initial tumor (cm)			
<6	40		55.6
≥6	32		44.4
Initial KPS			
<80	4		5.6
≥80	68		94.4
MIB-1 index (%)			
Median	3		
IDH mutation			
Mutation	42		58.3
Wild-type	30		41.7
Loss of 1p/19q			
1p/19q codeletion	15		25.0
1p deletion	24		40.0
19q deletion	23		38.3
Initial radiotherapy			
+	58		80.6
-	14		19.4
Initial chemotherapy			
ACNU	44		61
TMZ	2		3
None	26		36
PFS (years)			
Median		5.8	
Overall survival (years)			
Median		10.3	